The Data Processing to Detect Correlated Movements in Cerebral Palsy Patients in Early Phase

Okmin Pyon

Thesis submitted to the faculty of the Virginia polytechnic Institute and State University in partial fulfillment of the requirement for the degree of

Master of Science

In

Mechanical engineering

Chair: Alfred L. Wicks

Andre A. Muelenaer

John P. Bird

Dec 7th 2015

Blacksburg, VA

Key word

- Celebral parsy, Bilateral coordinated movement, Short time Fourier Transform, Accerelometer, Fidgety movement, Pediatric

The Data Processing to Detect Correlated Movement of Cerebral Palsy Patient in early phase

Okmin Pyon

Abstract

The early diagnosis of CP (Cerebral Palsy) in infants is important for developing meaningful interventions. One of the major symptoms of the CP is lack of the coordinated movements of a baby. The bilateral coordinated movement (BCM) is that a baby shows in the early development stage. Each limb movement shows various ranges of speed and angle with fluency in a normal infant. When a baby has CP the movements are cramped and more synchronized.

A quantitative method is needed to diagnose the BCM. Data is collected from 3-axis accelerometers, which are connected, to each limb of the baby. Signal processing the collected data using short time Fourier transforms, along with the formation of time-dependent transfer functions and the coherence property is the key to the diagnostic approach. Combinations of each limb's movement and their relationship can represent the correlated movement. Data collected from a normal baby is used to develop the technique for identifying the fidgety movement. Time histories and the resulting diagnostic tool are presented to show the regions of the described movement. The evaluation of the transduction approach and the analysis is discussed in detail.

The application of the quantitative tool for the early diagnosis of CP offers clinicians the opportunity to provide interventions that may reduce the debilitating impact this condition has on children. Tools such as this can also be used to assess motor development in infants and lead to the identification and early intervention for other conditions.

Index term- Accelerometer, fidgety movement, cerebral palsy diagnostic symptoms, coherence, short time Fourier transform, weighted average of window function.

Table of Contents

List of Figures and Tables

1 Introduction

1.1 Background to problem

Cerebral Palsy (CP) is a neurological disorder caused by a non-progressive brain injury or malformation that occurs while a child's brain is developing. [1]The main symptom is the difficulty of body movement and muscle coordination. There are a couple of methods which can diagnose CP. If CP can be diagnosed earlier than the current techniques allowed, there is some evidence that early intervention may improve the long-term outcomes. This research focuses on the method to detect one of the symptoms of CP, the lack of general movements (GM) of the baby.

CP mainly affects the body movement. Most of the patients experience difficulty in walking, involuntary movement, muscle rigidity and problems with coordination [2].CP is caused by brain injury before, during or after the birth of a baby, so the early detection of these symptoms are main keys for better care and treatment. In Chapter 2, detailed benefits of early detection and intervention will be discussed. This research can provide an early detection method of CP.

One of the major symptoms of CP is developmental delay [1]. There is a growth chart for developmental evaluation in table 2.2 [3]. For example, at three to four months, a baby can reach for toys. This chart can be used as a diagnostic tool as well as provide milestones for slow starters who will 'catch up.' However, CP diagnoses takes time. There are several processes to diagnose CP. The baby can be diagnosed soon after birth, but for the majority of cases, diagnosis can be made in the first two years [1]. The average age of diagnosis for a child with CP is 18 months. If the early diagnosis is possible, early intervention can support the child who will 'catch up' to the normal development phase earlier. Also early detection can help to find the benefits to offset the cost of raising a child with cerebral palsy. This new method which uses the BCM makes it possible to engage early intervention.

The financial aspect of CP was studied in ““Economic Costs Associated with Mental Retardation, Cerebral Palsy, Hearing Loss, and Vision Impairment – United States, 2003.” [4]Because CP needs continuous medical care, treatment and social support during lifetime, the expenses of the family is one of the serious issues. Here is the expense data for a person lifetime. [4]

Of the $921,000 estimated per person expense of cerebral palsy:

Indirect costs – 80.6%, or approximately $742,326.
Direct medical costs – 10.2%, or $93,942.
Direct non-medical costs – 9.2%, or $84,732.

This cost increases when the patient has severe symptoms and dependency to maintain a quality of life. Therefore, a family needs financial support. According to the same study in 2003, the national expense for the CP was a total of up to $11.5 billion. If doctors can provide an early intervention and the patient can have a highly independent life, the expense will decrease. This is the reason why early detection is necessary for a family experiencing CP. [4]

1.2 Background to signal processing approach

There are two ways to detect CP: brain scanning and expert observation. Because CP is caused by brain injury, CP can be diagnosed by brain scanning such as CT scans and MRIs [1] .Also a trained expert can observe the lack of GMs of a baby and diagnose CP, and other related diseases caused by brain damage. However, this training takes time and there are fewer experts than are needed. In addition, this method is less accurate than brain scanning because of the potential for human error. There are a couple of existing methods that studied CP diagnosis based on the GMs: Prechtl’s assessment [5]and computer-based video analysis (CBV) [6]

GMs are a part of the spontaneous movements until the baby is 6 months old. [5] GMs involve the whole body in a variable sequence of arm, leg, neck and trunk movement. [5]Prechtl defined abnormal GM as an indication of CP as following; “Two specific abnormal GM patterns reliably predict later cerebral palsy: 1) a persistent pattern of cramped-synchronized GMs. The movements appear rigid and lack the normal smooth and fluent character. Limb and trunk muscles contract and relax almost simultaneously. 2) The absence of GMs of fidgety character. So-called fidgety movements are small movements of moderate speed with variable acceleration of neck, trunk, and limbs in all directions. Normally, they are the predominant movement pattern in an awake infant at 3 to 5 months.” Trained experts can observe these movements and can diagnose brain damage from lack of GMs, specifically fidgety movement. In this research, it is hypothesized the relationship between limbs will be coordinated on xyz axis and can specify the GM by signal processing.

Figure 1.1 explains the GM classification according to the infant age by Prechtl [5]. As shown below, following the growth of the infant after birth, the infant shows the featured movements, General Movement., right after birth. From birth to week 5, an infant should show writhing movement. From 5 weeks to 20 weeks after birth, in normal development, the infant shows so called ‘Fidgety movement’ which demonstrates smooth and various rotation of each limb of the infant. Finally, after this period, the infant can control the limbs intentionally and move against gravity. Figure 1.2 shows how the deficient quality of these GMs relates to the outcome especially to the brain damaged syndromes like CP. Though the entire prognosis from deficient GMs quality was not directly connected to the CP, it is highly related to the motor disorder symptoms.

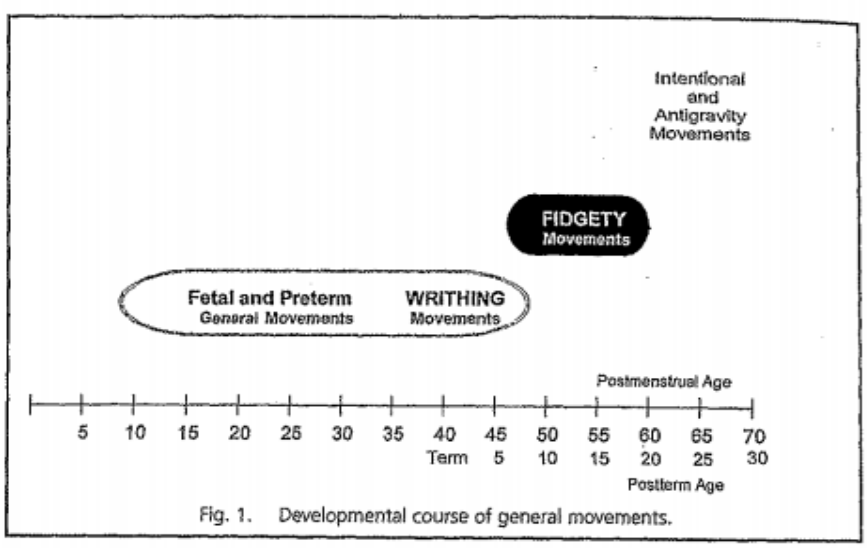

Fig. 1. Developmental course of general movements.

Figure 1.1 General movement development

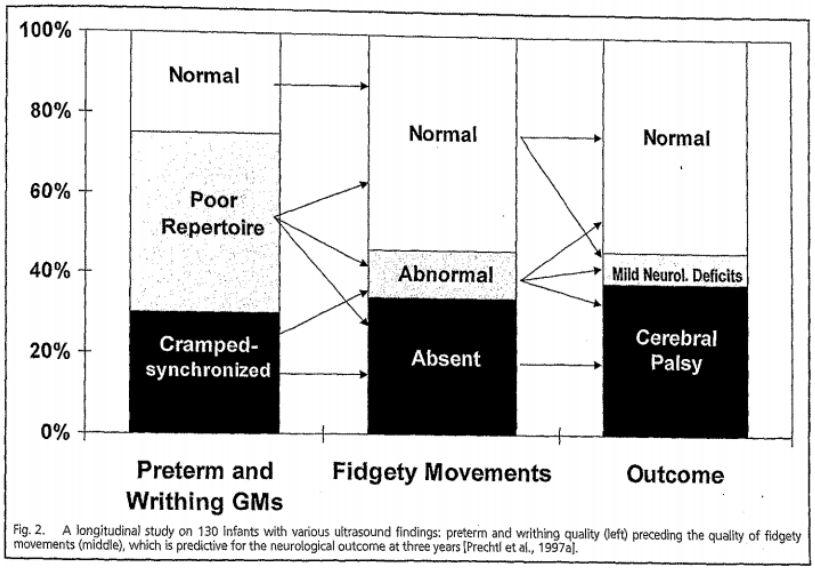

Fig. 2. A longitudinal study on 130 infants with various ultrasound findings: preterm and writhing quality (left) preceding the quality of fidgety movements (middle), which is predictive for the neurological outcome at three years [Prechtl et al., 1997a].

Figure 1.2 Relationship between abnormal GMs and its outcome

Prechtl's assessment of GM showed the high relationship between the lack of the Fidgety movement and CP. The researchers recorded the quality of the GMs in different ages of infants. In addition, they tracked the history of CP symptoms if a baby showed poor GM. Therefore, they could predict the later development of CP at a much earlier age than previously possible. In addition, the qualitative assessment of GMs could be possible without brain scanning at earlier age.

The CBV method compared the movement patterns between healthy babies and the babies with CP symptoms. They converted the recorded video of body movement of the babies into pixels from each frame of the video and compared the pixel area qualitatively and quantitatively. However, there is still low prediction rate (19.7%) to predict a future CP patient [5]. These two approaches to diagnose CP from lack of fidgety movement will be discussed in detail in chapter 2.

Therefore, the lack of fidgety movement is the main key to detect CP without brain scanning methods. The fidgety movement depends on the baby's limb movements which should demonstrate variety in speed and rotation. Therefore, we had an idea that the attachment of accelerometers to each of the infants' limbs would capture the movement of infants.

1.3 Problem statement

The purpose of the thesis is to develop and validate a signal processing technique that can be used to track the coordinated motion in developing post term infants. It has been suggested that tracking this development process may provide a quantitative assessment of infant coordinated movement development leading to a possible early diagnosis of brain damage associated with CP.

The goals of this paper are to find an appropriate signal processing method to evaluate the correlated movement of the baby automatically through these following points:

-Relationship between GMs and CP diagnosis
-Diagnostic methods and coordinated for movements of the infant
-Difference between stationary and non-stationary data in terms of signal processing

-Classical analytic methods for stationary (time invariant) data
-Time-frequency analysis for non-stationary data
-Coherence analysis in terms of time-frequency method
-Time-frequency coherence analysis of generated correlated data
-Time-frequency coherence analysis of acquired data of coordinate movements from accelerometers
-Time-frequency coherence analysis of acquired data from the infant
-Future opportunity

It is known that healthy baby's movements become more coordinated gradually as the baby grows. Before 6 months, this coordinated movement is typically not exhibited. FM at this stage is less correlated, or less coordinated among the limbs.

The signal processing method to evaluate the coordinated movement is generated from a computer based program and applied this method to the sample signals which are collected from accelerometer. Finally, this method was compared and validated to real data collected from the infant.

The novel method to assess fidgety movement automatically without trained experts and it showed highly reliable result by literature review. [7] This method can be expanded to the other diseases related to the motor disturbance. In addition, there is a possibility that accelerometers can be replaced with wearable smart devices which include accelerometers and gyroscopes.

In the treatment of CP, there is need for early detection and an affordable diagnostic tool. One of the major symptoms of CP is lack of general movements in the early development of baby. This movement signals can be acquired by accelerometers and analyzed by signal processing. We expect this new method can assess correlated movements of GMs and help to detect CP in early phase.

1.4 Organization of the thesis

This thesis is organized by the following 5 chapters.

Chapter 1:

Introduces the definition of the CP and the background of the need for early detection and early intervention of CP. The diagnostic methods and the main idea where this research originated are introduced. The GM categorize the development of the normal baby and lack of the fidgety movement indicates the high possibility of CP syndrome. Overall, chapter 1 introduces the background to understand the goals and principles findings of this thesis.

Chapter 2 :

Explains more details of the causes and the symptoms of CP. Bilateral coordinated movement, which demonstrates the correlated movement between limbs is discussed, and the related research which explains the relationship of the lack of the coordinated movement and CP is introduced. Other signal processing approaches to detect CP automatically in early phase are discussed and compared to the time frequency method. Chapter 2 provides the literature review which defines the symptoms of CP, signal processing techniques and backgrounds.

Chapter 3 :

Examines and discusses the mathematical theory of the research. Auto spectrum and cross spectrum with regard to the time-frequency analysis are defined. The correlated motion and the signal that came from the motion can be quantified by coherence analysis. The researcher generated data from Matlab and verified the idea of coherence with respect to expected time-frequency method. Chapter 3 explains the principle theory of signal processing for generated correlated signal from a computer based program, Matlab.

Chapter 4 :

Applies the signal processing technique verified in chapter 3 to the real data collected from accelerometers. The hardware system to acquire the signals is introduced and examined in this chapter. The correlated movement simulating the baby's limb movement was generated in a different perspective. The result based on these signal data is presented and discussed. From this result, the researcher can define the correlated movement between limbs. Chapter 4 applies the new signal processing method to the real data from accelerometers and compares the result to the expected result.

Chapter 5 :

Discusses the results from chapter 4 to the CP diagnosis and showed the possibility of applying this signal processing technique to the other diseases which have motor disturbance symptoms. Also, hardware improvement suggestions are listed with an explanation of how this finding can be beneficial to the CP diagnoses. Chapter 5 summarizes results and discusses the future possibilities of the findings.

2 Literature Review

Cerebral Palsy (CP) is a syndrome described by loss or impairment of motor function which is caused by brain damage. The brain damage is caused by brain injury or abnormal development of the brain that occurs while a child's brain is still developing before birth, during birth, or immediately after birth. Cerebral palsy affects body movement, muscle control, muscle coordination, muscle tone, reflex, posture and balance. It can also influence fine motor skills, gross motor skills and oral motor functioning [1]. According to the current data for cerebral palsy, 1 out of 250 [1] newborn infants have CP [1].

2.1 Cerebral Palsy (CP)

CP is not a disease but it is a syndrome which is caused by brain damage at any birth stage. This brain injury can happen in the developing fetus, as well as during and after the birth. The Table 2.1 explains the main causes of the brain damage which can cause CP. These causes can include a bleeding in the developing brain and deficiency of oxygen. [8]

Table 2.1 The main causes of CP

Phase of development	Causes
Before the birth	prenatal disinfection(especially first 3months), radiation treatment, drug addiction, placenta disorder, umbilical cord disorder, and anoxi during pregnancy
During the birth	premature baby, respiratory obstruction, and amniotic fluid infection
After the birth	head injury, infection(encephalitis, meningitis) and brain tumor

For the case of CP, the brain damage itself will not be expanded to the other part of the brain or worsen after it happened, but the symptoms will be changed with the growth of the infant. The perfect medical treatment of CP does not exist, but there are many treatments which can help patients to live independently with a quality of life. The infant with CP can get support by the following development chart in Table 2.2 [9] which indicates the cognition and motion control tasks at each stage after birth. The research shows promise of better life quality with the earlier treatment. [9] Therefore, the early diagnose of CP is the necessary task to initiate the early intervention.

2.2 Diagnosis techniques

The early engagement for the treatment of CP can help patients to have less complications and promise better life quality in the future. To attain early intervention and diagnosis of CP, it is necessary to perform the physical examinations: brain CT(computerized tomography), brain MRIs(magnetic resonance imaging), EPS(evoke potential study) and electroencephalography. Also, a detailed medical history of the infant can provide information related to brain damage.

CP is rerely correctly diagnosed in infants younger than 12 months old because these examination devices cannot be correctly used for infants. “For all the benefits of early diagnosis, delayed diagnosis does occur – predominantly because the disorder is difficult to diagnose and doctors worry about the impact on parents. Receiving a diagnosis of cerebral palsy can be devastating, and doctors fear parents may withdraw and further hamper the child’s development.” [10] However, the signs of development like crawling, standing when supported and pointing to things can be a milestone, as described in Table 2.2. If these expected signs are not observed, the infant has trouble controlling all of their limbs, or a lack of vitality, parents are recommended to see a doctor. Also severe jaundice of the newborn, as well as an abnormal history of birth and early birth can be signs of risk to CP.

An infant with CP may have some delays in development. For example, there are some signature movements the infant is supposed to show in normal developmental phases: controlling head (3months), sitting independently (6 months), crawling (8 months), standing holding object (8 to 12 months), and walking independently (12-17 months). [3] Most of babies with CP have delayed motion controls in each phase in the development chart.

Table 2.2 Development Milestone of 1yr old baby in movement, physical development and cognition [3]

Movement and physical development	Cognitive
Gets to a sitting position without help Pulls up to stand, walks holding on to furniture (“cruising”) May take a few steps without holding on May stand alone	Explores things in different ways, like shaking, banging, throwing Finds hidden things easily Looks at the right picture or thing when it’s named Copies gestures Starts to use things correctly; for example, drinks from a cup, brushes hair Bangs two things together Puts things in a container, takes things out of a container Lets things go without help Pokes with index (pointer) finger Follows simple directions like “pick up the toy”

Also, when the infant with CP can walk independently, standing and running posture are observed under the effects of abnormal coordination. Pediatricians can confirm CP under these symptoms with the help of technical examinations: brain scanning, MRIs, CT, neurological examination and blood testing. Other than abnormal gestures due to the neurological disorders, the infant with CP can experience accompanied symptoms like intelligence disorder, epileptic seizure, visual impairment and other symptoms. However, the most obvious symptom of CP is motor disturbance.

From Prechtl’s paper [5], motor disturbance also affects the infant by showing deficient Fidgety movements which is the one of the stages in the General Movement

(GM). “General movements are part of the spontaneous movement repertoire and are present from early fetal life onwards until the end of the first half a year of life. GMs are complex, occur frequently, and last long enough to be observed properly. The limbs are wax and wane in intensity, force and speed, and they have gradual beginning and end. Rotations along the axis of the limbs slight changes in the direction of movements make them fluent and elegant and create the impression of complexity and variability. If the nervous system is impaired, GM loses their complex and variable character and become monotonous and poor.” [5]

By Prechtl, 2002, [5] there are multi- stages in GM. “from the many distinct movement patterns appearing during the course of development from fetus to young infant. (Figure 1.1), at 6 to 9 weeks’ post-term age, are called writhing movement [Hopkins and Prechtl, 1984].” [10] “Writhing movements are characterized by small to moderate amplitude and by slow to moderate speed. Typically they are elliptical in form.” [5]

“At 6 to 9 weeks’ post-term age, GMs with a writhing character gradually disappear and whereas fidgety GMs gradually emerge” [10, 5]. Fidgety movements are present up to the end of the first half a year of life when intentional and anti-gravity movements start to dominate. “Fidgety movements are of small amplitude, moderate speed, and variable acceleration of neck, trunk, and limbs in all directions continually in the awake infant except during fussing and crying. The quality of GMs is probably modulated by corticospinal and reticulospinal pathways and, hence can be affected by impairments of these structures. Therefore, if there is under damage related to brain and neurological system, GMs will be also affected.” By Prechtl’s [5], “If fidgety movement are never observed from 9 to 20 weeks post-term, we call this abnormality “absence of fidgety movement”, The absence of fidgety movements is highly predictive for later neurological impairment: particularly for CP” [10] [5] figure 2.1 represent how absence and abnormality of GMs can be related to CP and other mild neurological deficits.

Under the circumstances we discussed, the early diagnosis of CP is the one of the most important keys to start early intervention. The analysis of GMs can provide the

earlier clinical practice guidelines (CPGs). This method is a more economical diagnostic tool compared to the other brain scanning diagnostic methods. Currently, the average CP diagnosis with brain scanning techniques takes up to 18 months [1]. However, in figure 1.2, critically, the absence of FM can predict future CP for infants younger than 6 months.

2.3 Signal processing approaches

"Qualitative assessment of GMs is totally non-intrusive, easily learned, and cost-effective". [5] Also the quality of FM can be judged by trained experts within only 5-10 minutes [5].This GMs assessment skill can be obtained by training. "There a standardized basic and advanced training courses, lasting 4 to 5 days are provided by the General Movements Trust" [11] In 2015, we have many experts who completed the training for GMs assessment. However, compared to the occurrence of CP as 1 out of 250 newborn babies in United States, we need more objective assessment method than the current subjective method for GM. Gestalt perception, which is the guideline for GMs assessment, still relies on the observer's subjective decision. There is a high risk regarding consistency due to the prejudice of the observers. For better quality of the diagnosis for CP, we need an unbiased and objective GMs assessment method.

There are a couple of approaches to evaluate FM automatically as anon-subjective method. For example, there are two research studies, one of which dealt with video assessment and the other used accelerometers. [12] [13]. These two approaches attempted to quantify the quality of FM.

The first study title is 'Using computer-based video analysis in the study of fidgety movement'. The research showed the video assessment to detect FM patterns to relate the patterns for CP. The general movement toolbox (GMT) is a quantitative tool which originally came from music gesture toolbox (MGT). MGT is a tool for calculation and filtering of motion images of the recorded moving object in the camera. (Figure 2.1). The researchers advanced this MGT to GMT to find a pattern in absence of FMs. The researcher could extract motiongram, which describes movement comparison results

frame by frame. After this procedure, the researchers set a regression model, and assessed FMs quantitatively. Consequently, the absence of FMs showed low mean quantitative value and higher variability of the centroid motion in the motiongram. 2 out of 82 babies under this study were referred to the pediatric clinic because the absence of FMs was recorded. After 2 years of follow-up studies, these two babies had neurological issues. However, only 2 subjects for the statistical research had limitations and there is difficulty to find and to get enough statistical data due to the limited subjects with CP.

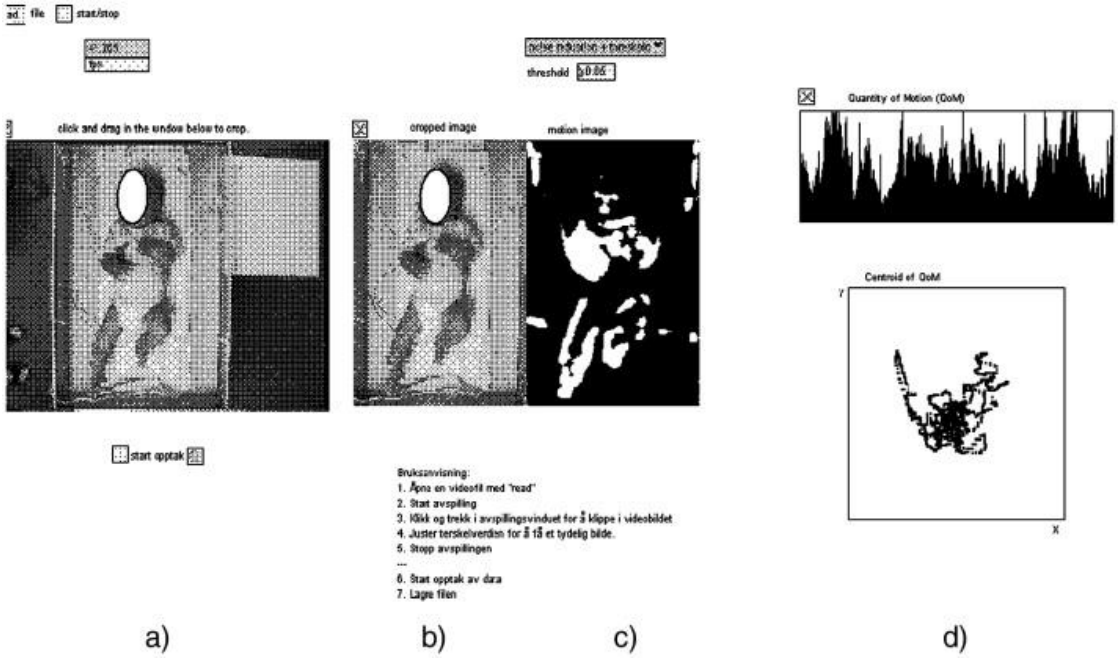

Figure 2.1 GMT captured and calculated image

Table 2.3 Between-group differences between present and absent FMs in variables derived from the GMT.

	Present FMs (110)	Absent FMs (27)	Between-group differences	
	Mean (SE)	Mean (SE)	*p*-value	95% CI
Q_{mean}(%)	2.95 (0.15)	1.79 (0.17)	< .001	(0.71, 1.62)
Q_{max}(%)	32.70 (1.87)	29.04 (2.70)	.269	(− 2.92, 10.24)

Q_{SD}(%)	3.20 (0.13)	2.41 (0.17)	< .001	(0.37, 1.22)
Cx_{mean}	4.65 (0.06)	4.49 (0.15)	.328	(− 0.17, 0.50)
Cy_{mean}	4.31 (0.06)	4.01 (0.17)	.107	(− 0.69, 6.73)
C_{SD}	2.17 (0.05)	2.82 (0.10)	< .001	(− 0.09, − 0.04)
V_{SD}	6.35 (0.18)	8.29 (0.42)	< .001	(− 2.86, − 1.01)
A_{SD}	1.03 (0.03)	1.35 (0.07)	< .001	(− 0.48, − 0.17)

Q_{mean} = quantity of motion mean; Q_{max} = quantity of motion maximum; Q_{SD} = quantity of motion standard deviation; Cx_{mean} = centroid of motion in *x*-direction mean; Cy_{mean} = centroid of motion in *y*-direction mean;C_{SD} = centroid of motion standard deviation; V_{SD} = velocity standard deviation; A_{SD} = acceleration standard deviation.

The next research [13] is used for the statistical analysis for FMs. The researcher used 6 sensors: 4 limbs, and head and torso of the subject. Each sensor can provide a placement information as xyz coordinate. Based on the signals coming from these sensors, the absence of GMs appeared as monotonous signal with a lack of variation. Therefore, it showed a more periodic appearance. The researcher quantified the FM patterns with different parameters with autoregressive and moving average model (ARMA). Figure 2.2 and Figure 2.3 represent the analytic methods used to quantify the FMs. The signals came from both normal and abnormal babies at 25Hz sampling frequency. Varying window size K, the study differentiated the area the signal value from the moving average value from normal and abnormal cases. The other statistical methods were applied with standard deviation Figure 2.3. The second method used the original approach of Moving Average (MA), but it also considered areas off from the standard deviation. Finally, the researcher used severability statistically to find the FM features. The distance between the signal and the MA and its occurrence was considered as an important parameter. The statistical method needs parameters which can comprehend FMs. Thus, the author changed those parameters to get the optimal classification result.

At the optimal settings of parameters, he got 90% specificity and 86% sensitivity in studies of 81 subjects to find absence of FMs. The researcher showed statistical methods to classify FM with sensors and left the result open to future research about clinical applications.

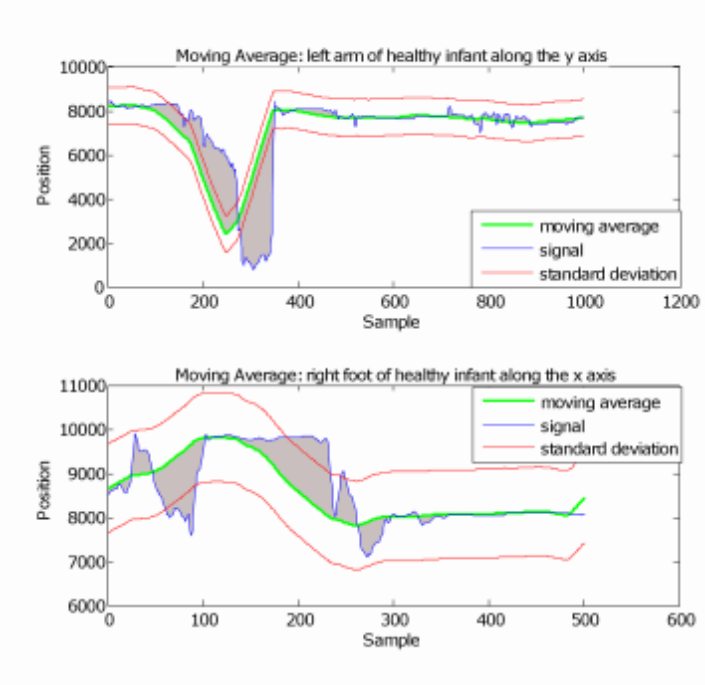

5a: Normal

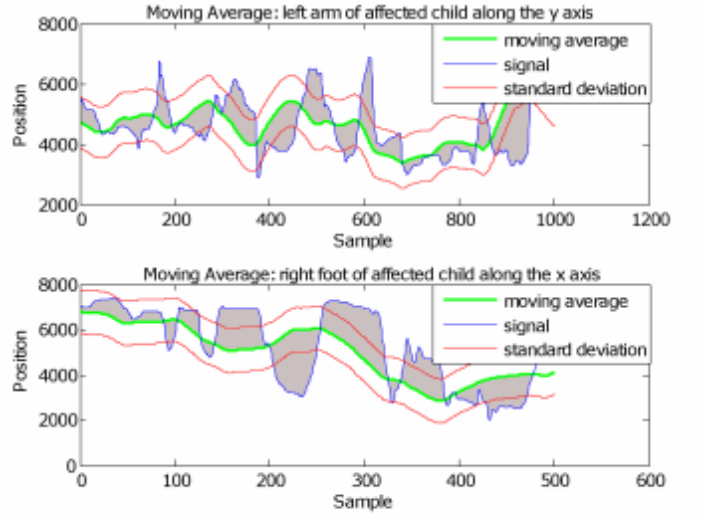

5b: Abnormal

Figure 2.2 The comparison signal which represent normal to abnormal GM using MA.

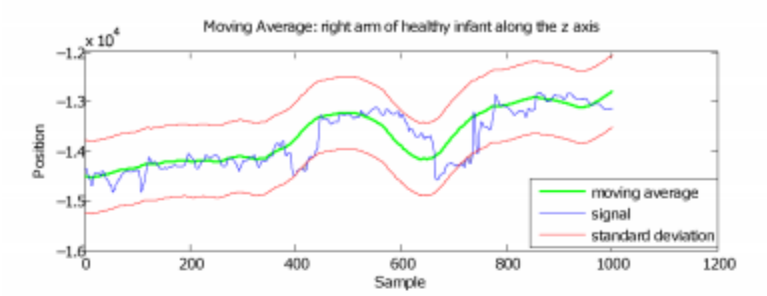

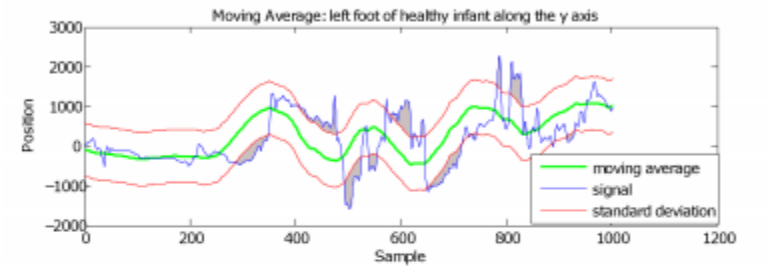

6a: Normal

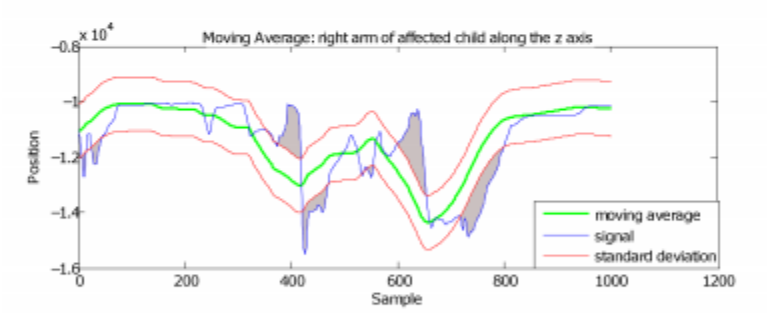

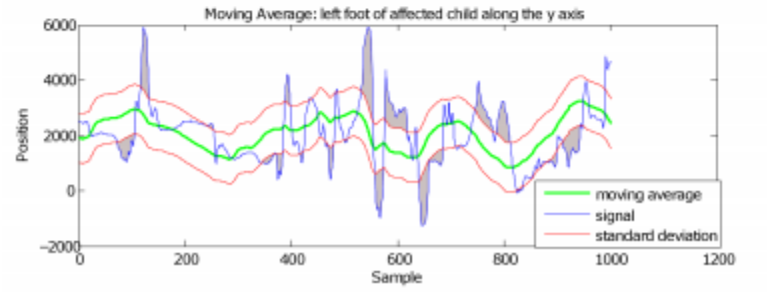

6b: Abnormal

Figure 2.3 The comparison signal which represent normal to abnormal GM using MA with standard deviation.

In this research, it was assumed that the symmetric motor disturbance so called bilateral movements would be gradually changed according to the brain development. It

means that the limbs will move in correlation with each other. Most of the babies with CP have trouble controlling the limbs relatively. Therefore, the researcher expected that the bilateral coordination would be continuously changing during the FM stage. And in the study of “Efficacy of Constraint-Induced Movement Therapy for Children With Cerebral Palsy With Asymmetric Motor Impairment. Edward Taub, Sharon Landesman Ramey, Stephanie DeLuca, Karen Echols”, [7] the researcher studied about constrained induced (CI) movement therapy. The main point of the paper is that how CI can affect infant with CP according to their ages. It was shown that the early intervention affects their future quality of life and independency. In the paper, the researcher said “impaired hand function is a major disability in children with hemiplegic cerebral palsy (CP). As a result, children with hemiplegic CP often fail to use the involved upper extremity and learn to perform most tasks exclusively with their noninvolved upper extremity (ie, developmental disuse).” Therefore, they lack controllability of symmetric correlated movement, so called bilateral coordinate movement can imply high possibility of brain damage.

2.4 Time frequency response analysis

In this research, FM was assumed as the correlated changes in brain development. The FMs represent gradual movement with various speeds and different angles. If the uncorrelated movement disappears with growth, the brain and the nervous system are attaining functionalities to control the limbs. The discrimination of FM will be presented by using a frequency response (FR) approach with moving average (MA). Because FM does not occur constantly over time (non-stationary), the limbs’ correlated movement with respect to time change is influenced. The signal processing in the time frequency method will be discussed in detail in the next chapter to evaluate signal’s characteristic according to the time changes.

3 Theory

As introduced above, the characteristics of FMs and brain development in the neurological system is highly related to the spontaneous limbs' movement of the infants. Also in the statistical ARMA model in the literature review, the torso and the neck sensor does not affect recognitions of the GMs. Therefore, it is safe to say that the coordinated motions are highly related to the brain development without consideration of neck and torso movement. The relationship label between the limbs can be represented as correlation in time domain, or coherence in frequency domain. Both time domain and frequency domain with the moving average of time will be considered. This research assumed that the high coherence would represent the limbs' coordinated movements of the infants. Before applying the signal processing method to the data acquired from the infant, the generated signals which the characteristics of the signal is already known will be analyzed as time- frequency method to the generated signals.

3.1 Frequency domain and time domain

In the signal-processing point of view, the signal is presented in the time domain or frequency domain. The signal in time domain shows the changes in respect of time, also the signal in frequency domain shows the signal's amplitude with respect of the frequency. In other words, the frequency domain shows the characteristics of the signal in frequency point of view. These two different domains can be transferred by using Fourier transform (FT), and the transfer equations is shown underneath. [Equations 3.1] and [Equations 3.2] are the classical Fourier transform pair. Continuous representation is bounded by $\pm\infty$, therefore it requires the signal to be bounded. It cannot be applied to the real data. Transitioning to discrete sampled data requires the additional assumption of periodicity.

Continuous-continuous FT

$$X(f) = \int_{-\infty}^{\infty} x(t) e^{-j2\pi ft} dt \quad (3.1)$$

$$x(t) = \int_{-\infty}^{\infty} X(f) e^{j2\pi ft} dt \quad (3.2)$$

When acquiring a signal, one of the most important features the researcher should care about is the difference between the continuous and discrete (or digital) feature. For collecting data from a digital device, even those with the most advanced and the highest sampling frequency, the data must be discrete. In other words, real data is always discrete. Only in the ideal case, the continuous data can be acquired from the sample with sampling frequency as infinity. Therefore, in the real data, the Fourier transform in the discrete time and discrete frequency will be applied. This transfer equation is shown underneath. The transform is called as fast Fourier transform (FFT) or discrete Fourier transform (DFT). In the paper, all transforms used FFT to find the frequency characteristic of the data.

Discrete-discrete FT

$$X_k = \int_{n=0}^{N-1} x_n e^{j2\pi(mF)(nT_s)} = \sum_{n=0}^{N-1} x_n W^{mn} \quad (3.3)$$

$$x_n = \frac{1}{N} \sum_{m=0}^{N-1} X(mF) e^{j2\pi(mF)(nT_s)} = (\frac{1}{N}) \sum_{m=0}^{N-1} X(mF) W^{-mn} \quad (3.4)$$

$$where, W = e^{j2\pi(FT_s)} = e^{-j2\pi/N}$$

For example, sinusoidal signal with frequency as f_0=1Hz was generated, $y = \sin(2\pi t)$. The generated signal has the sampling frequency f_s = 50Hz. By Shannon's or Nyquist theorem, the sampling frequency should be larger than twice of the original signal's frequency. Therefore, f_s =50Hz can be considered as high enough for sampling frequency. Figure 3.1 represents the signal in the time domain and in the frequency

domain. The frequency domain signals include the real part, imaginary part and modulus value of the signal.

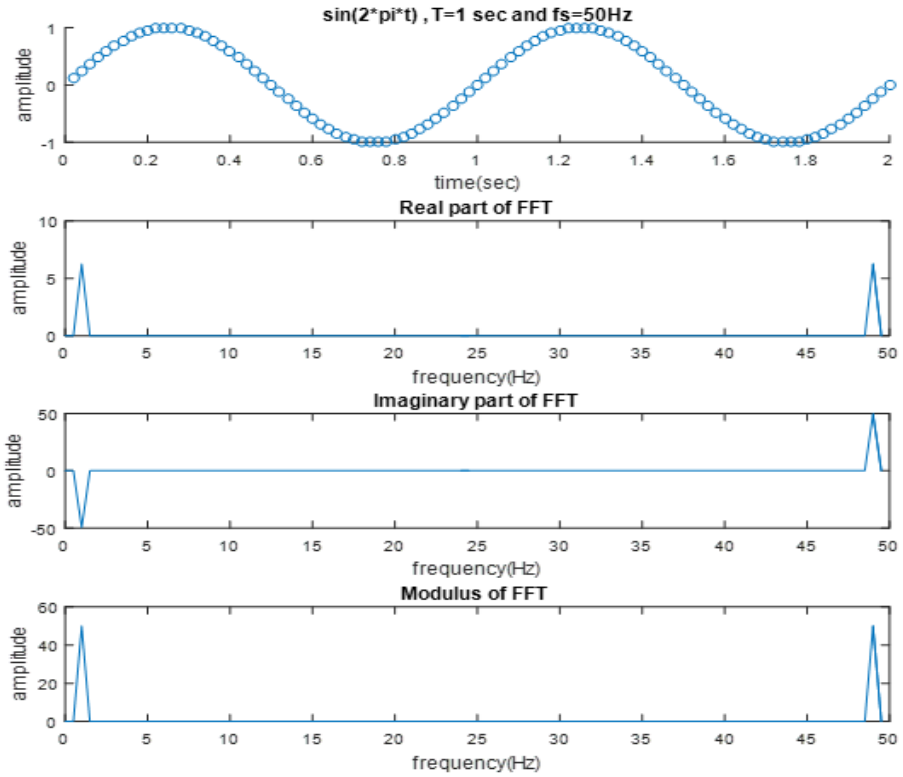

Figure 3.1 Sinusoidal signal of 1Hz in time domain and Fourier transformed response in frequency domain

3.2 Stationary model analysis

The relationship between the signals can be represented as correlation in time domain. In the time domain, if the input and output are the same, the correlation is called as auto-correlation. If the input and output signal are different, the correlation is called as cross correlation. The equations is shown below and it has τ as time convolution,

Auto correlation for continuous model,

$$R_{xx}(\tau) = E\{x(t)x(t+\tau)\} = \lim_{T\to\infty}(\frac{1}{2T})\int_{-T}^{T} x(t)x(t+\tau)dt \qquad (3.5)$$

Auto correlation for discrete model,

$$R_{xx}(k) = \lim_{N\to\infty}(\frac{1}{2N})\int_{n=-N}^{N} x_n x_{n-k} \quad (3.6)$$

Cross correlation for continuous and discrete

$$R_{xy}(\tau) = E\{x(t)y(t+\tau)\} = \lim_{T\to\infty}(\frac{1}{2T})\int_{-T}^{T} x(t)y(t+\tau)dt \quad (3.7)$$

$$R_{xy}(k) = \lim_{N\to\infty}(\frac{1}{2N})\int_{n=-N}^{N} x_n y_{n-k} \quad (3.8)$$

Figure 3.2 shows the autocorrelations of white noise and sinusoidal wave @1Hz. Every signal shows highest correlated values at τ =0 sec in time domain in autocorrelation. In the same manner for the frequency domain, if the input and the output signals are the same, it is called as auto spectrum. If the input and the output are different, cross-spectrum is used to see the relationship in the frequency domain. The auto spectrum and cross spectrum in frequency domain will be used in detail in the later part of this chapter. Because of the convolution, cross spectrum is not commutative. Therefore, $G_{xy} \neq G_{yx}$.

$$R_{xx}(t) \leftrightarrow G_{xx}(f), R_{xx}(t) = \int_{-\infty}^{\infty} G_{xx}(f)e^{j2\pi ft}df \quad (3.9)$$

$$R_{xy}(t) \leftrightarrow G_{xy}(f), R_{xy}(t) = \int_{-\infty}^{\infty} G_{xy}(f)e^{j2\pi ft}df \quad (3.10)$$

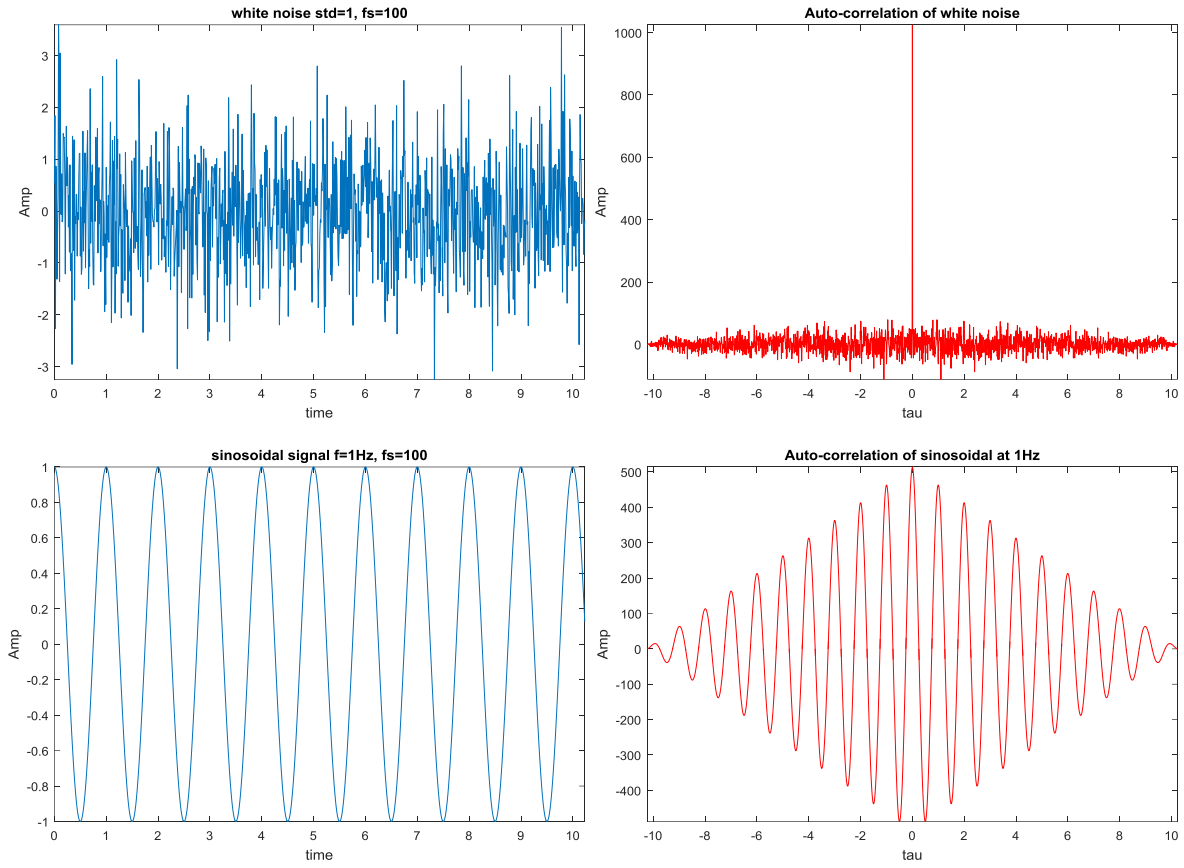

Figure 3.2 Autocorrelations of a white noise and the 1Hz sinusoidal wave from the right signals

3.5 Coherence estimation

Coherence show the relativeness between two signals in frequency domain. An output signal came from an input was generated, and the output is the filter result from LPF in Figure 3.3. In the ideal case, it was assumed that the signal does not have noise. The output signal totally depends on the input before the cutoff frequency f_c. This dependency can be quantified in the frequency domain by coherence analysis. There are two equations to get the coherence, but they are eventually the same.

Coherence in frequency domain

$$\gamma^2(f)=\frac{G_{yu}(f)G_{uy}(f)}{G_{uu}(f)G_{yy}(f)}=\frac{G_{yu}(f)G_{yu}{}^{*}(f)}{G_{uu}(f)G_{yy}(f)}=\left(\frac{\left|G_{yu}(f)\right|^2}{G_{uu}(f)G_{yy}(f)}\right) \quad (3.11)$$

Coherence is always bounded as $0\le\gamma^2(mF)\le 1$, $\gamma^2(mF)$=1 means completely correlated and $\gamma^2(mF)$=0 means completely uncorrelated. However, in the finite real data in the discrete domain, the 'averaging' is needed to get the meaningful coherence

$$\gamma^2(f)=\frac{G_{yu}(f)G_{uy}(f)}{G_{uu}(f)G_{yy}(f)}=\frac{\frac{1}{L}X(f)^{*}Y(f)\cdot\frac{1}{L}Y(f)^{*}X(f)}{\frac{1}{L}X(f)^{*}X(f)\cdot\frac{1}{L}Y(f)^{*}Y(f)}=1$$

by this equation of

(3.12). $X(f)$ and $Y(f)$ are the DFT forms of $x(t)$ and $y(t)$ for entire time block accordingly.

$$\gamma^2(f)=\frac{G_{yu}(f)G_{uy}(f)}{G_{uu}(f)G_{yy}(f)}=\frac{\frac{1}{L}X(f)^{*}Y(f)\cdot\frac{1}{L}Y(f)^{*}X(f)}{\frac{1}{L}X(f)^{*}X(f)\cdot\frac{1}{L}Y(f)^{*}Y(f)}=1 \quad (3.12)$$

Total length of the data is L and the coherence result in the real discrete data are always unity because the numerator and denominator terms are the same in equation

$$\gamma^2(f)=\frac{G_{yu}(f)G_{uy}(f)}{G_{uu}(f)G_{yy}(f)}=\frac{\frac{1}{L}X(f)^{*}Y(f)\cdot\frac{1}{L}Y(f)^{*}X(f)}{\frac{1}{L}X(f)^{*}X(f)\cdot\frac{1}{L}Y(f)^{*}Y(f)}=1$$

(3.12). Therefore, it is necessary to take an average to evaluate the relevant coherence. The coherence equation with averaging over k time block equations is indicated below

$$\gamma^2(f)=\frac{G_{yu}(f)G_{uy}(f)}{G_{uu}(f)G_{yy}(f)}=\frac{\frac{1}{L}X(f)^{*}Y(f)\cdot\frac{1}{L}Y(f)^{*}X(f)}{\frac{1}{L}X(f)^{*}X(f)\cdot\frac{1}{L}Y(f)^{*}Y(f)}=1$$

(3.12).

$$\gamma^2(f)=\frac{G_{yu}(f)G_{uy}(f)}{G_{uu}(f)G_{yy}(f)}=\frac{E[X_k(f)^{*}Y_k(f)]\cdot E[Y_k(f)^{*}X_k(f)]}{E[(X_k(f)^{*}X_k(f)]\cdot E[Y_k(f)^{*}Y_k(f)]} \quad (3.13)$$

$E[X_k(f)^{*}Y_k(f)]$ is the average the components.

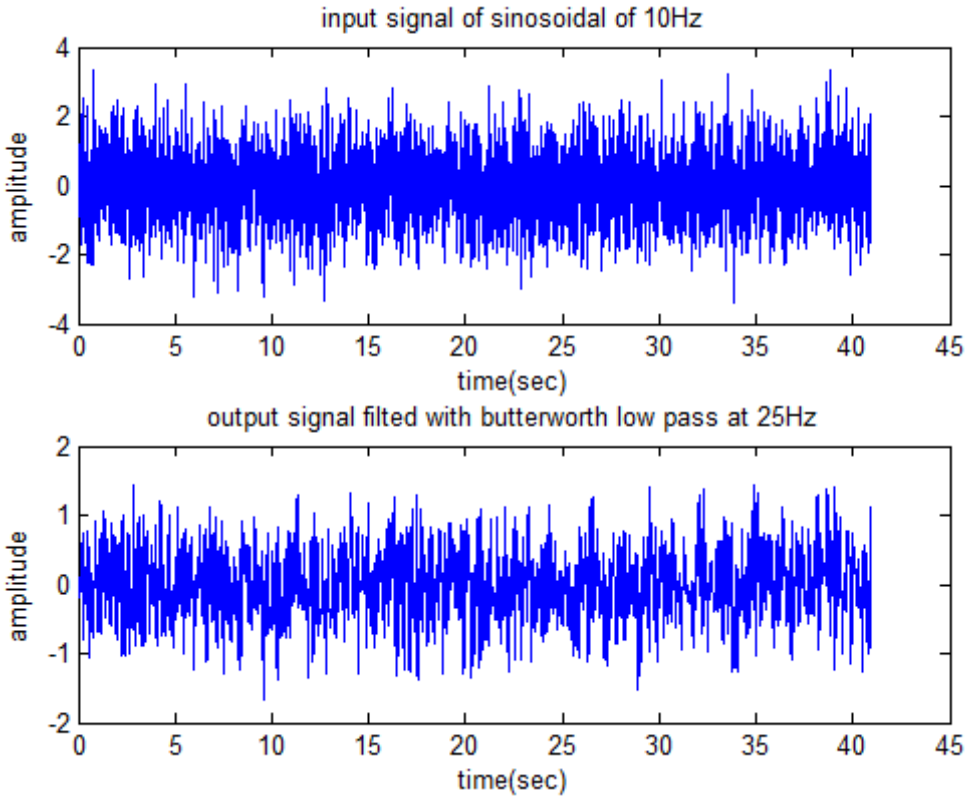

Figure 3.3 Two highly correlated signals, output signal is the filtered signal with Butterworth LPF @ 25Hz.

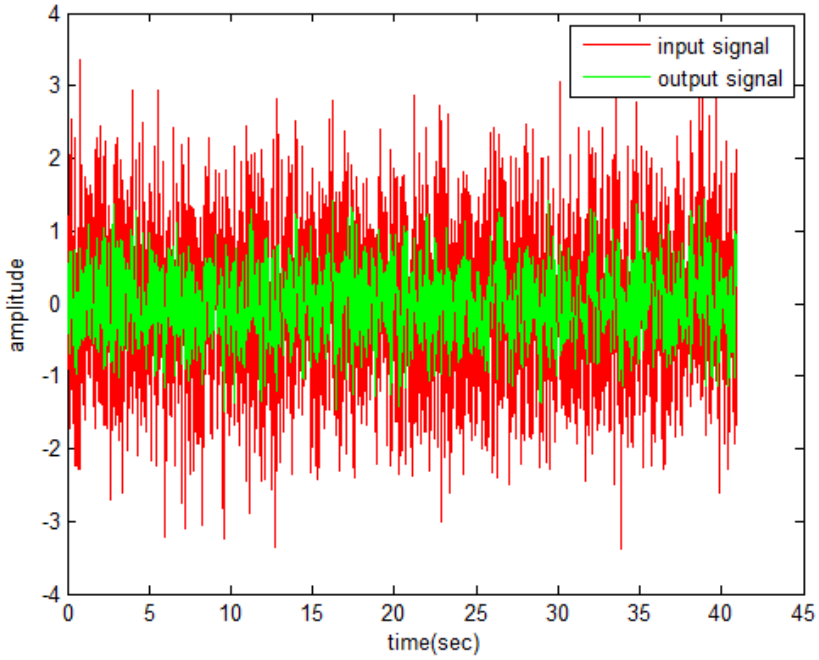

Figure 3.4 Red: Input signal with white noise and 10Hz sinusoidal, Green: filtered input signal from 6th order LPF @ 25Hz

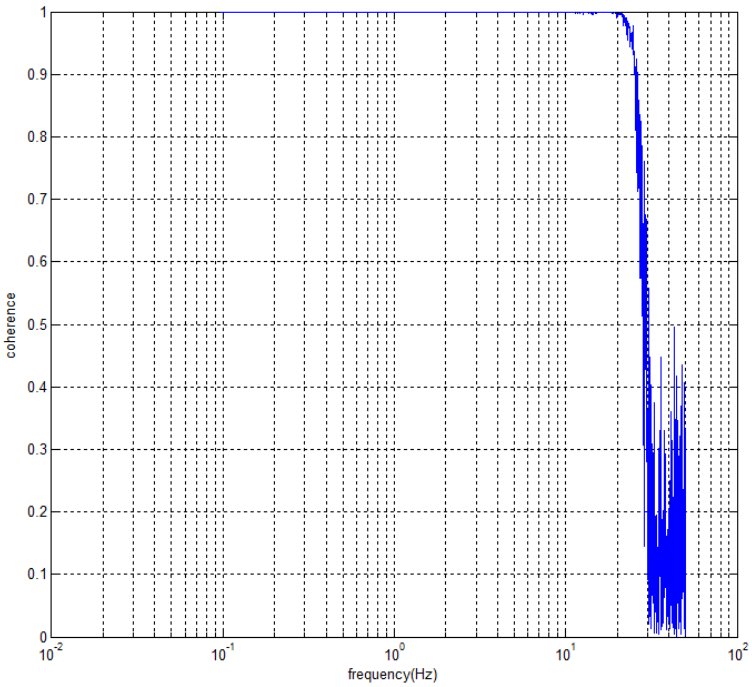

Figure 3.5 Coherence plot showing unity = 1 till 25Hz, which is the cut off frequency by 6th order Butterworth filter.

In this paper, it is important how the infant's limbs move related each other according to the time changes. With STFT, the coherence between two signals with respect to time and frequency can be attained. The coherence value will be calculated continuously along the time changes to see the limbs' correlation in the later chapter.

3.3 Frequency Response Function (FRF) Review

Frequency response function, also called FRF, shows the relationship between two signals like the input signal and the output signal in the frequency domain.

Convolution in time is output. A linear system can be defined by the convolution of the impulse response of the system with the input. Rather than performing the time domain convolution of the signal, it is significantly computationally easier to transform the input signal and output signal into the frequency domain where the relationship now becomes a multiplication problem. FRF is defined as [Equation 3.5] and the FRF

estimator H1 can be used also, by the assumption that we have no noise in the input signal.

Continuous and discrete FRF equation

$$Y(f) = H(f) \cdot X(f) \Leftrightarrow y(t) = \int_{-\infty}^{\infty} h(t) \cdot x(t-\tau) d\tau \qquad (3.14)$$

Discrete-Discrete FRF equation

$$Y(f) = H(f) \cdot X(f) \Leftrightarrow y[n] = \sum_{k=-\infty}^{\infty} h[k] x[n-k]$$

$$H(f) = \frac{G_{xy}(f)}{G_{xx}(f)} = \frac{G_{yy}(f)}{G_{yx}(f)} = \frac{Y(f)}{X(f)} = \frac{X^*(f)Y(f)}{X^*(f)X(f)} \qquad (3.15)$$

Or

$$H_1(f) = \frac{G_{xy}(f)}{G_{xx}(f)} \qquad (3.16)$$

$$H_2(f) = \frac{G_{yy}(f)}{G_{xx}(f)} \qquad (3.17)$$

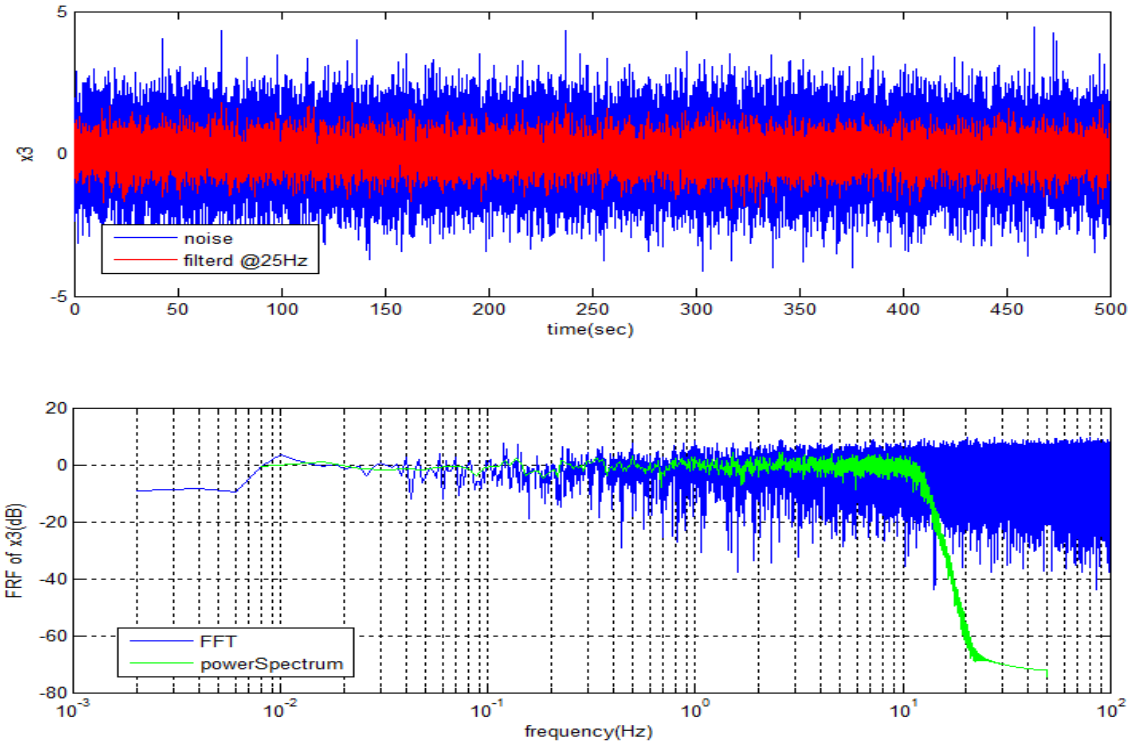

Figure 3.6 Top: blue is the white noise at standard deviation =1, red is filtered white noise fc= 25Hz. Bottom: FRF of Butterworth LPF at 25Hz

The Figure 3.6 shows the FRF of the filtered signal from low pass filter (LPF). The generated white noise and the filtered through LPF for the entire time range were compared. Therefore, in the frequency range after f_c=25Hz, FRF would be reduced because of the LPF. The green line shows the expected characteristics of the FRF.

3.4 Time frequency review

This FRF signal processing can be useful for the stationary data or a time invariant case, which means that the data for the entire time has a common characteristic like top plot of the Figure 3.9. In other words, for non-stationary data, some features of the signal only presents in a specific time section in the acquired signal like in the bottom plot of the Figure 3.9. In the Figure 3.9, the top is the stationary sinusoidal

signal at f_0=10Hz and the other is the non-stationary signal which has white noise component only until N=0 to N=2^{11}. After N= 2^{11}, it has the same sinusoidal wave with the stationary plot of f_0 =10Hz. Both signals are sampled at 100Hz and number of sample is N=2^{12}=4096. The non-stationary data have the different signals before N=2^{11}=2048. Frequency changing functions of time. For FRF in entire time section, the white noise component placed first half of the signal will reduce the response at 10Hz compared to separated time section method. Therefore, it is required to separate the signal into two time sections and it will produce FRF between input and output according to the time changes. The FRF result of entire time section is shown in Figure 3.12 and Figure 3.13.

GMs will be observed in specific time section inconsistently. It is safe to assume that the GM has the characteristic of a non-stationary signal and GM will be changed according to the growth of the infant, so the frequency response analysis with respect to the different time sections is necessary to find the relationship of the limbs. This analysis is called time frequency analysis.

Coherence demonstrates the correlated movements in frequency domain. However, the issue arisen from the classical method is that the coherence analysis can be useful in the stationary data only (the time invariant case). The infant does not show a constant or continuous movement. However, the infant moves only when she or he likes to move. Accordingly, the researchers need to analyze the response in certain time ranges when the infant shows significant movement. Therefore, the time frequency analysis technique can be helpful for a non-stationary signal. Figure 3.7 demonstrates the technique as flow chart and figure 3.5 shows the example of how the time-frequency method works. In figure 3.5, to simulate the real data acquired in chapter 4, the signal was assumed to be collected at fs=200Hz during 200secwith a sample length of N=40,000. This signal has different frequency features in different time sections, as non-stationary data. Thus, the normal coherence analysis could not be used to get the features of this signal because the entire time data was averaged to get the frequency response. Instead of calculating coherence on full data set, like in figure 3.5, coherence

was calculated for the first 50 seconds, N=10,000 . After the coherence of first block of data was calculated, the coherence of 91 blocks with 90% overlapping data were calculated, Figure 3.8 the next record data size of N=10,000 from N=100 to N=10100 was used to find the next coherence characteristic. The same schematic repeated until the end of data recorded. The coherence which represents the correlated signals according to time and frequency can be established by this signal processing method.

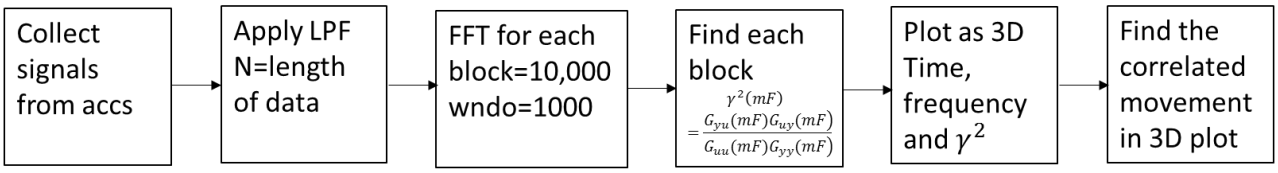

Figure 3.7 Flow chart of signal processing as time frequency analysis

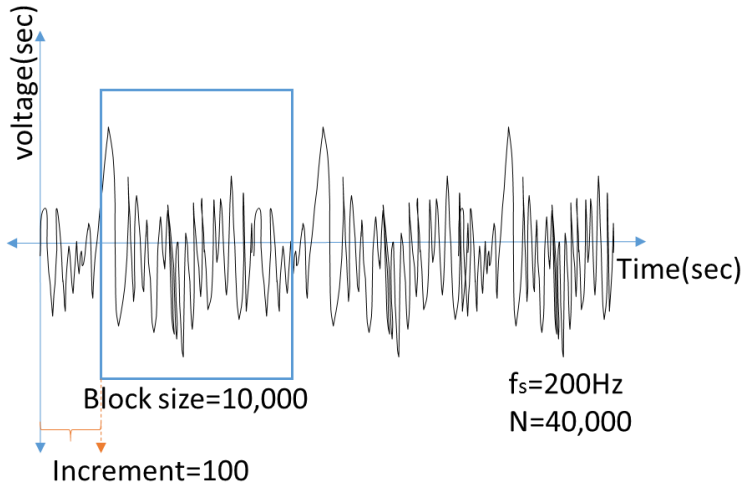

Figure 3.8 Signal processing example of time frequency analysis

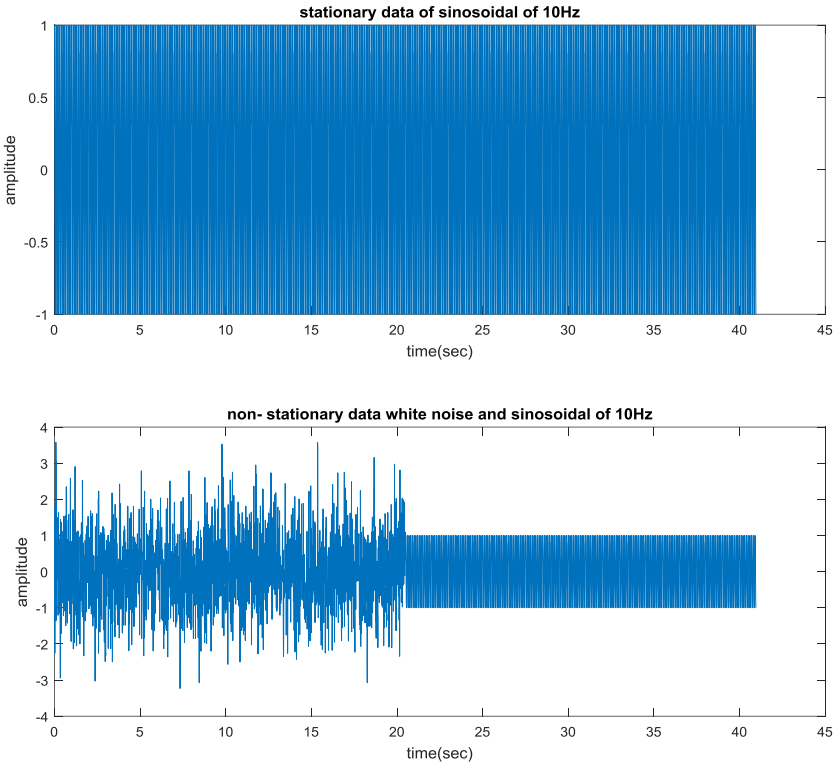

Figure 3.9 Stationary of sinusoidal signal of 10Hz and non-stationary data with white noise before 20 sec and same sine wave after 20sec

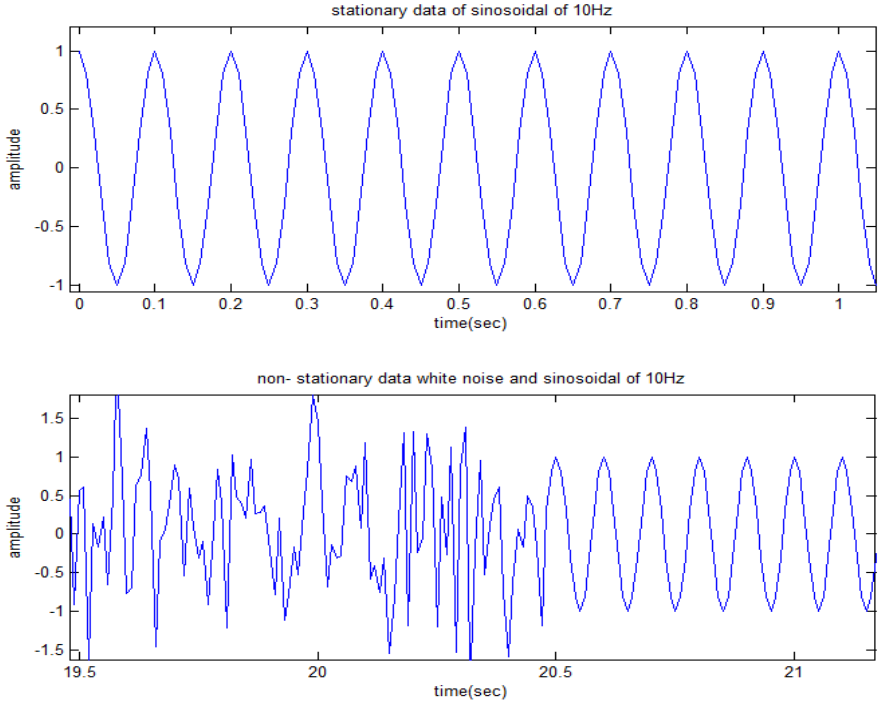

Figure 3.10 Zoomed Non-stationary signal in bottom and stationary signal on top.

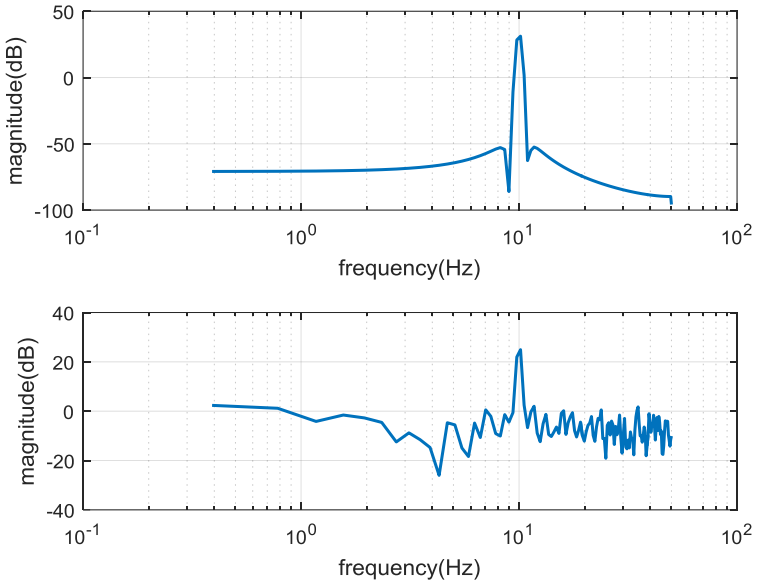

Figure 3.11 Auto spectrum of stationary and non-stationary data for entire time section

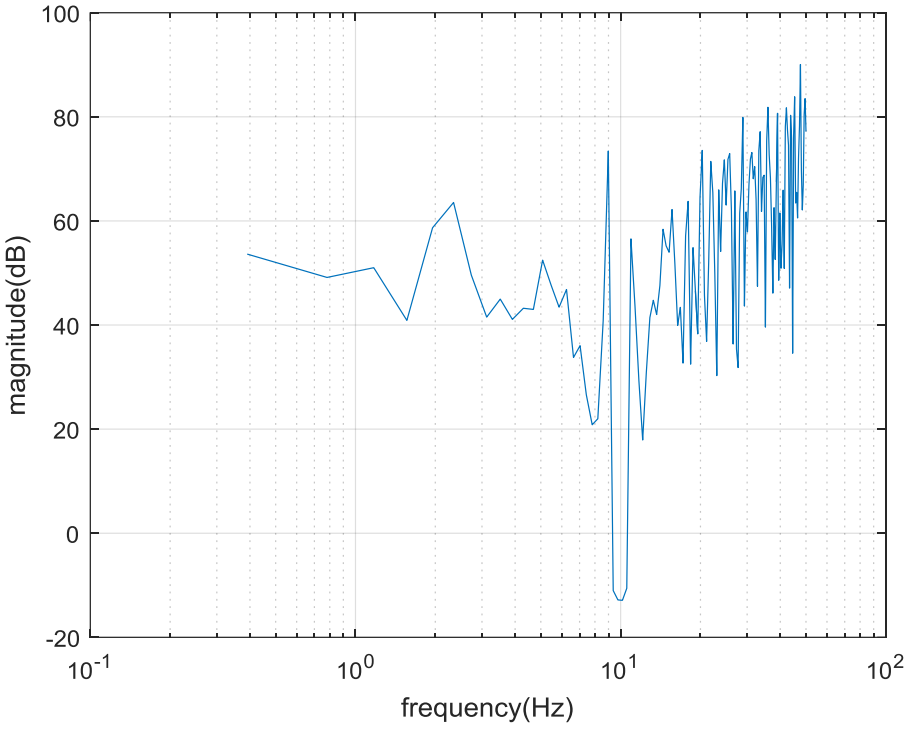

Figure 3.12 FRF of between these signals in dB for entire time section

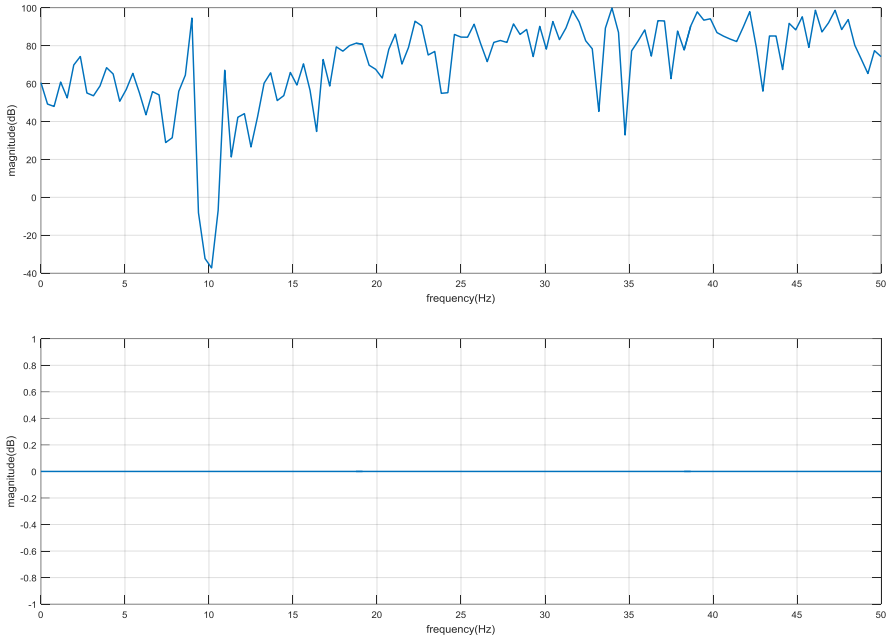

Figure 3.13 Time separated FRF in dB of between these signals before N= 2^{11} =2048 and after N= 2^{11}

The graph in Figure 3.12 shows that the entire time section FRF shows lower magnitude at 10Hz than Figure 3.12. Moreover, the entire time FRF does not represent that two signals after 5.12sec, N= $2^{11}$are the same. However, with the two separated section FRF, it does represent that after 5.12sec, N= 2^{11}, the input and output are the same. Figure 3.3 shows that the FRF between input and output is the same, 0dB after 5.12 sec.

In the Figure 3.13, for non-stationary data, FRF with respect to different time sections is necessary to see the frequency characteristics. The time section is called block size; the optimal size of the block will be discussed in the further section of this chapter and introduce short time Fourier transform, which can present the different size of block to transfer from time domain to frequency domain.

Accordingly, if a signal shows certain frequency characteristics in specific time, we need to extract those time sections and find the frequency characteristics as we did in Figure 3.13. Figure 3.9 represents that in the first half shows white noise and the other half shows 10Hz sinusoidal output. In the above, we can clearly see the different in the

pattern changes in the signal at 2^{11}. Thus the signal can be parsed as half at 2^{11}. However, generally, it is hard to find out the specific time where the frequency features show certain characteristic especially when the signal is mixed with multiple frequency components. In this case, it is needed to change the time section continuously and see the FRF result changes by the change of the time section. In Figure 3.13 shows the two different time section before and after N= 2^{11} because at this point, it was obvious change was observed where the pattern changes. For example, we could try to separate as four quarters in time section with reduced averaged block size. FRF in the various times section, window, it is so called as short time Fourier transform (STFT).

3.4 Short Time Fourier Transform (STFT) Review

The STFT is a signal processing technique which has both information about time and frequency domains. The common method to evaluate the relationship between two signals for entire time as whole is not valid for time-variant signal in this research. Therefore, the STFT which considers the signal as the locally stationary was suggested.

Continuous time STFT <-> time domain

$$X_t(f) = \int_{-\infty}^{\infty} e^{-j2\pi ft} x(t) h(t-\tau) dt \qquad (3.18)$$

Window function h is at time τ , and energy spectrum at time t and the frequency f is shown underneath,

$$S(t, f) = \left|S_t(f)\right|^2 = \left| \int_{-\infty}^{\infty} e^{-j2\pi ft} x(t) h(t-\tau) dt \right|^2 \qquad (3.19)$$

FRF in time-frequency analysis

$$H(f,t) = \int h(\tau,t) e^{j2\pi f\tau} d\tau \qquad (3.20)$$

$$y(t) = \int h(\tau,t) x(t-\tau) d\tau \qquad (3.21)$$

Defining the optimal size of the block and finding the frequency response of the block are important. Mostly, for normal baby's GMs, the frequency range cannot be exceed higher than 10Hz by estimation and observation in the lab. Through a brute force method and trial and error, we found that the block size of N=1000 is the most appropriate size for the process when f_s=200Hz.

Therefore, in case of the non-stationary data, to figure out the frequency component, moving average Fourier transform, STFR will be the useful. In addition, as discussed before, in the FRF, coordinated of movement of infant highly related to the coherence. To define this idea, in the last section of the chapter, the two highly correlated signals would be generated and the resulted coherence with respect to time and frequency will be presented in 3D plot using SFTF.

3.6 Time-frequency Coherence analysis

Two different signals were generated to observe the dependency with respect to time and frequency. For example, the input signal is the mixing of signals at 5Hz, 10Hz, 40 Hz and white noise. In this analysis, the sampling frequency is 400Hz to get a fine frequency resolution. Therefore, a signal which has higher frequency than 200Hz cannot be regenerated. (By Nyquist and Shannon's theorem). From the input signal, in the second quarter of the entire time, only 5Hz component pass through LPF f_c = 20 resulted to the output. The time frequency method expects the high coherence at second quarter of the time at 5Hz. With the same manner, the different input frequency characteristics pass through LPF according to four quarters time sections. The total number of sample is 2^{12} and every quarter, different frequency component can pass through LPF accordingly, white noise, 5Hz, 10Hz and 40Hz. In the time frequency signal process, high coherence at 5Hz, 10, 40Hz with respect to time will be expected. The noise in the input signal does not correlate to the output ideally. It means that the signal

noise came from one accelerometer does not correlated to the other accelerometer's noise when the signal is acquired through the accelerometer from the infant.

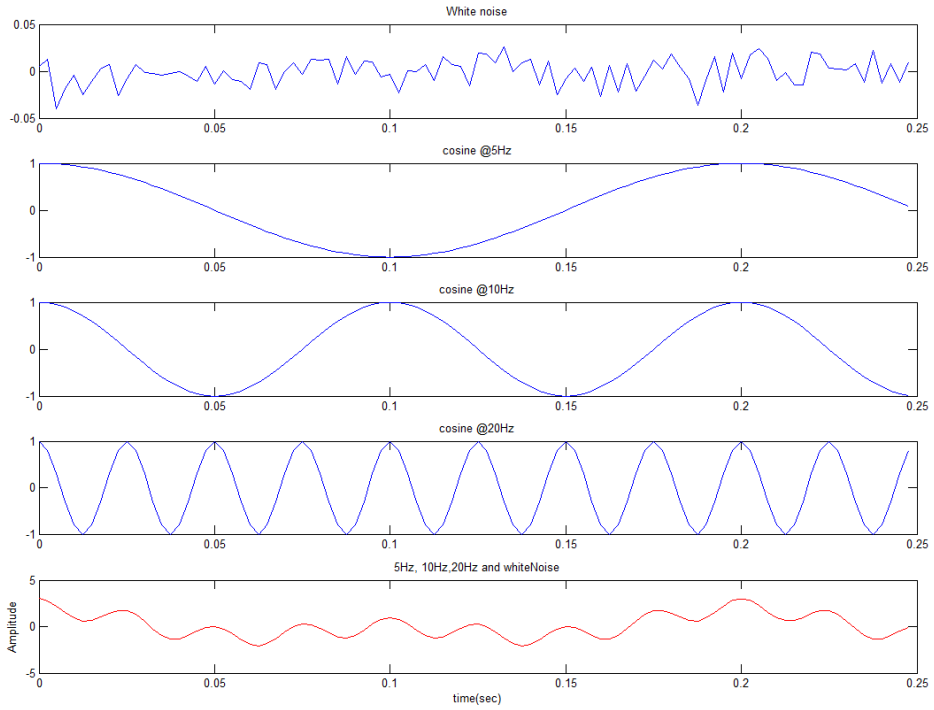

Figure 3.14 Input signals, red signal is combined of white noise, 5Hz,10Hz,40Hz , number of data N=2^{12}=4096

In the Figure 3.14, we can see that the input signal has high frequency component at 5Hz, 10Hz, and 40Hz as designed. The white noise presented in the entire frequency range. In the first quarter of the time section, 0~2.56sec , the filter passed only the white noise to the output, 2.56~5.12 sec passed 5Hz, 5.12~7.68 sec passed 10Hz, 7.68~10.24 sec passed 40Hz by using LPF @ cutoff frequency of 20Hz. So at each quarter of the time section, a different frequency feature would present as high coherence in FRF. Though the input is stationary data, the output came from filter has non-stationary as designed. If the coherence was evaluated for the entire time, Figure 3.17 will be shown. As seen, the high coherence peaks at expected time section at

expected frequency were unclear. Usually, higher than 0.7 coherence was considered as highly related signals.

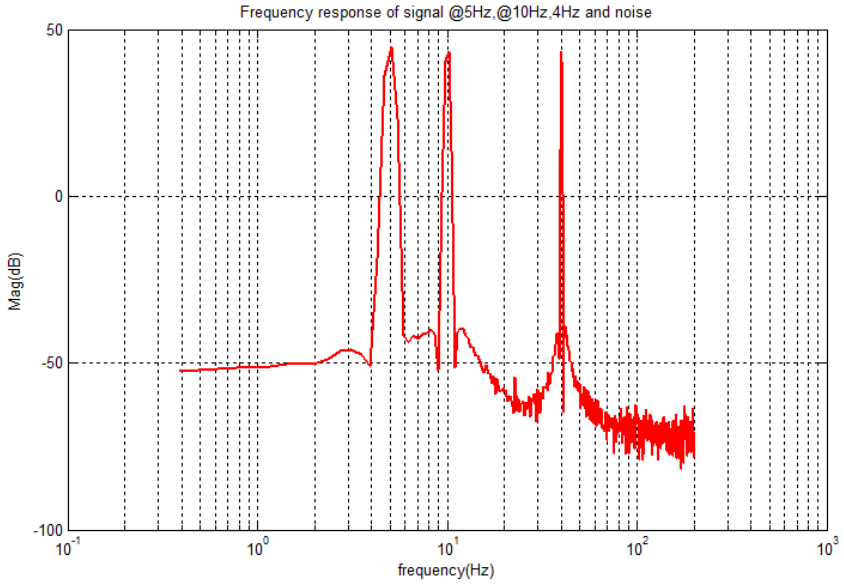

Figure 3.15 Auto spectrum of the input signal which is combined of white noise, 5Hz, 10Hz and 40Hz

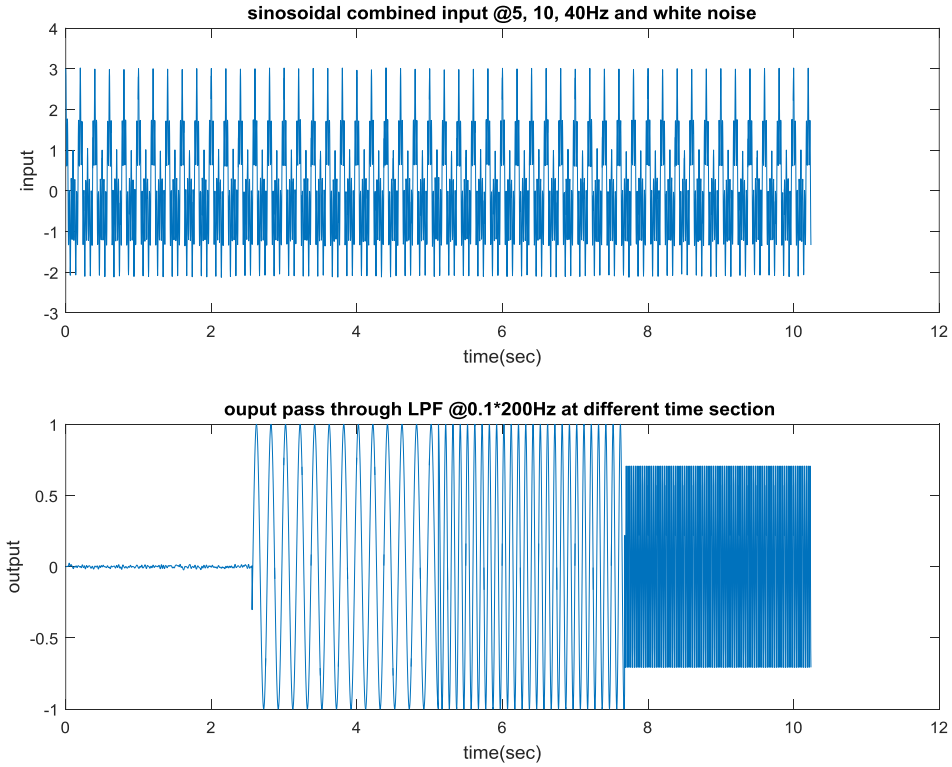

Figure 3.16 Input signals which has different frequency features as stationary and the output signals which has different frequency characteristic as non-stationary

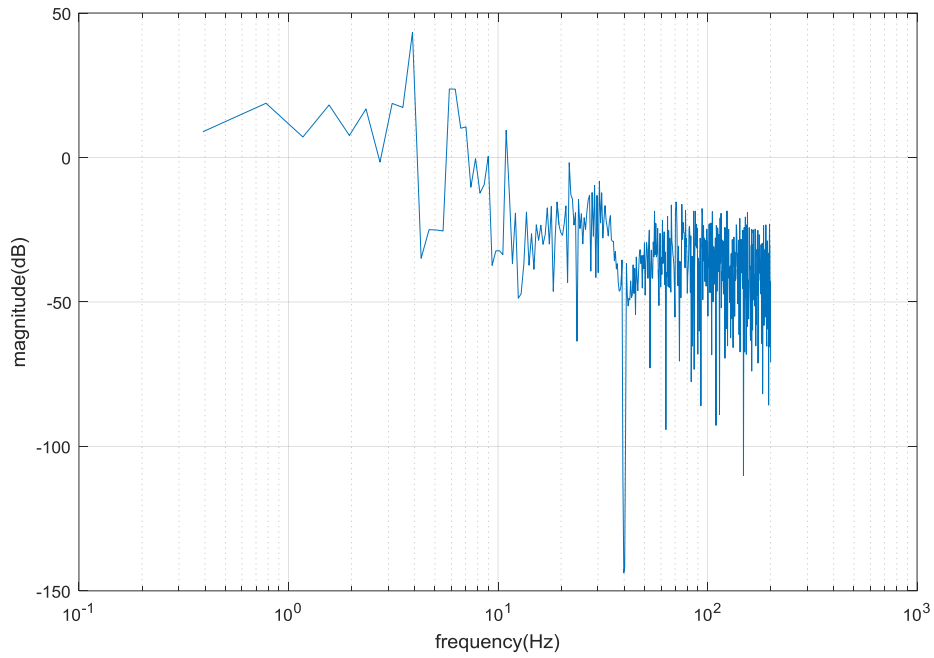

Figure 3.17 FRF, H1 estimation between input and output for entire time range

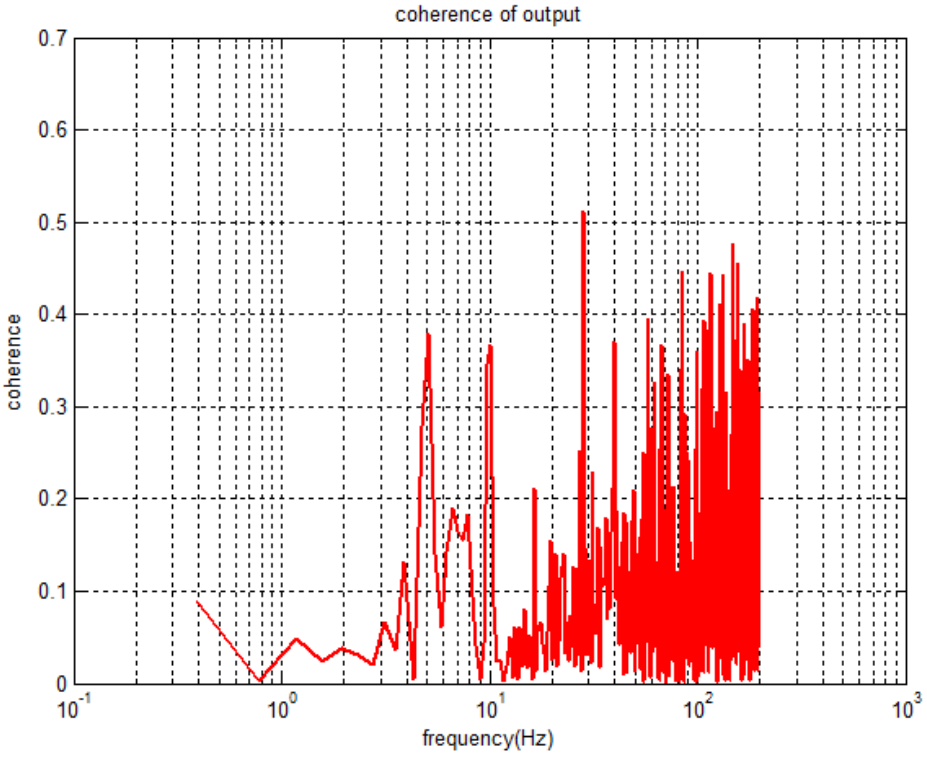

Figure 3.18 Coherence analysis for entire time range

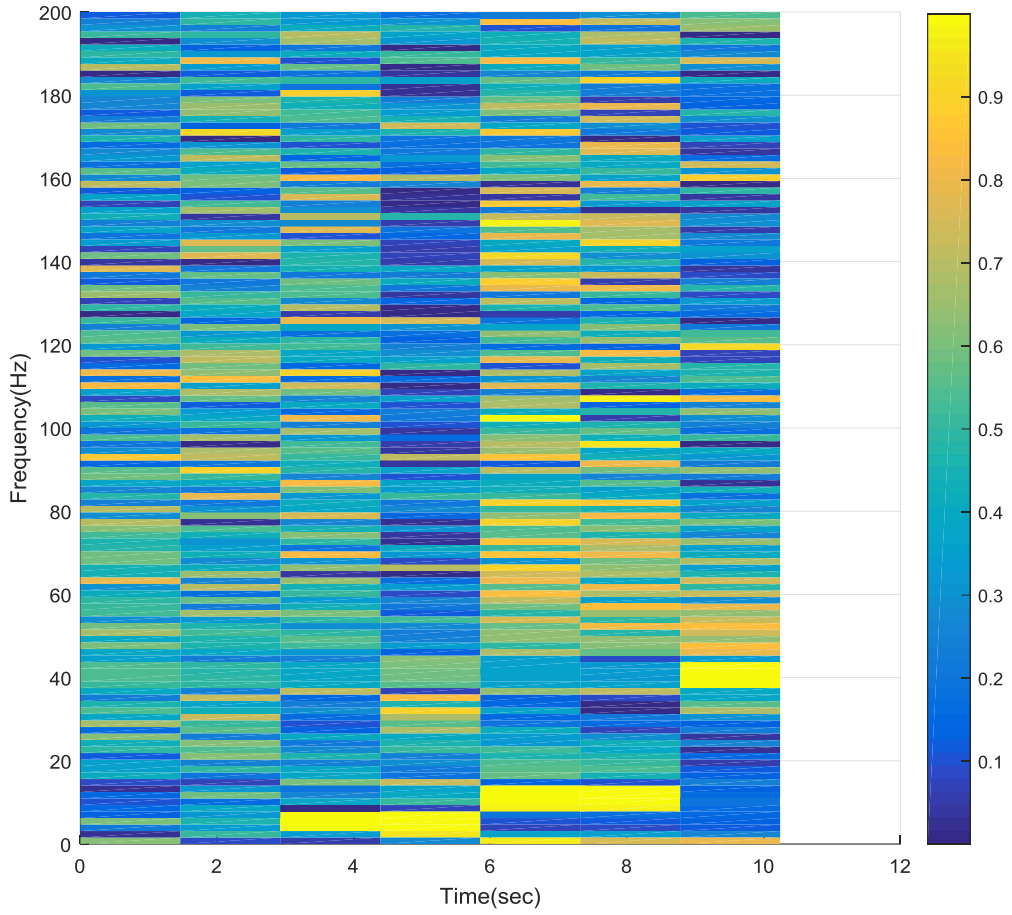

Figure 3.19 Time-frequency coherence analysis between input and output. Three frequency features of 5Hz, 10Hz, and 40Hz as designed in figure 3.16

When we are applying moving average with respect to time, the appropriate window size was 2^9 =512 sample data. From 3 to 6 at 5Hz, from 6 to 9 at10Hz, from 9 to10 at 40Hz shows the high coherence at 0.9~1 coherence. White noise consistently shows the low coherence. Unlike Figure 3.18, time frequency analysis shows the expected high coherence at the time and frequency as designed in Figure 3.19. The high coherence shows as yellow and the correlated signals was defined in the plot in y axis as frequency and in x axis as time. According to the original design, both input and output signals in the second quarter of the time and the 5Hz frequency region are highly correlated. The plot resulted as yellow block as the researcher expected. And the third quarter and the last quarter showed the same result as designed. The same method will

be applied to the real data from the accelerometers and the correlated signals will be generated from the accelerometers to apply the time frequency analysis.

4 Application to real data

As we discussed in chapter 3, the signals from two 3 axis accelerometers were acquired to verify the time frequency analysis to evaluate the correlated movements between the limbs of the infant. The signals were collected with sampling frequency of f_s=200Hz, and the size of the data bin N= 20,000. To generate correlated movements between the limbs, two accelerometers are attached to the researcher's each arm separately and the researcher moved both arms correlatively intentionally. During 3 minutes total, the signals were acquired. The first 1 minute was measured as calm and stationary, no movement the next 1 min was measured with correlated shaking (assumed less than 10Hz frequency) and the last minute was observed in correlated rotation change to get continuous x-y-z axis changes. The first 1minute was assumed that baby showed no movement at all. However, it does not mean that the transducer cannot capture any signal because the infant and the researcher who was simulating the stable movement cannot be 100% hold state. If the assumption and the analysis were correct, the high coherence peak at different frequency along each 1 min block time section would be observed.

4.1 Hardware and its testing

The device setting was evaluated for appropriateness. The data acquisition system was consisted of NI-9107 ADC, and MEMS accelerometer, MMA7331LC. The NI9107 with 12 bit ADC system works at $\pm$10V which means that least significant bit (LSB) of 4.9mV/bit

$$\frac{20}{2^{12}-1} = 4.9mV/bit$$

The supply voltage of the accelerometer system was 3.3V. With the supply voltage of 3.3V, the offset is 1.405V by the spec sheet. For the testing, the graph in Figure 4.1 shows the output voltages came from two accelerometers with no external force except the earth gravity. The first 20 seconds is for the adjustment period, adjusting the sensor. The resultant, vector sum voltage output from both accelerometers should be 2.63V for 1g from the spec sheet of 4G sensitivity and 3.3V supplied voltage. The data sheet states the characteristic of the MEMS accelerometer as Radiometricity, which means that the offset voltage and the sensitivity linearly scale with the supply voltage. Accordingly, the sensitivity according to the supply voltage, V= 3.3V is 319.375mV by spec sheet. The actual resultant voltage from accelerometer 1 was 2.66V and from the accelerometer 2 was 2.83V in figure 4.2. Ideally, by the datasheet, the ideal resultant voltage should be 2.63V under 1g gravity. The errors are 1.10% and 7.95% accordingly. These errors are still reliable because this research studies the dynamic correlate changes between the signals from accelerometer. In the later part of the chapter, the assumption will be verified.

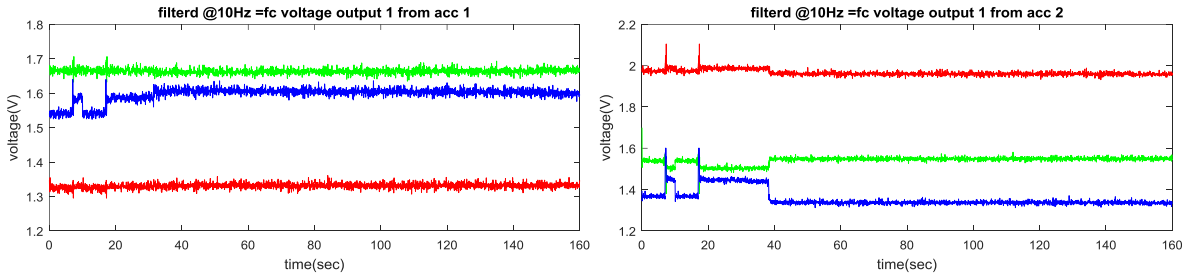

Figure 4.1 Voltage outputs from accelerometers without external force after 20sec

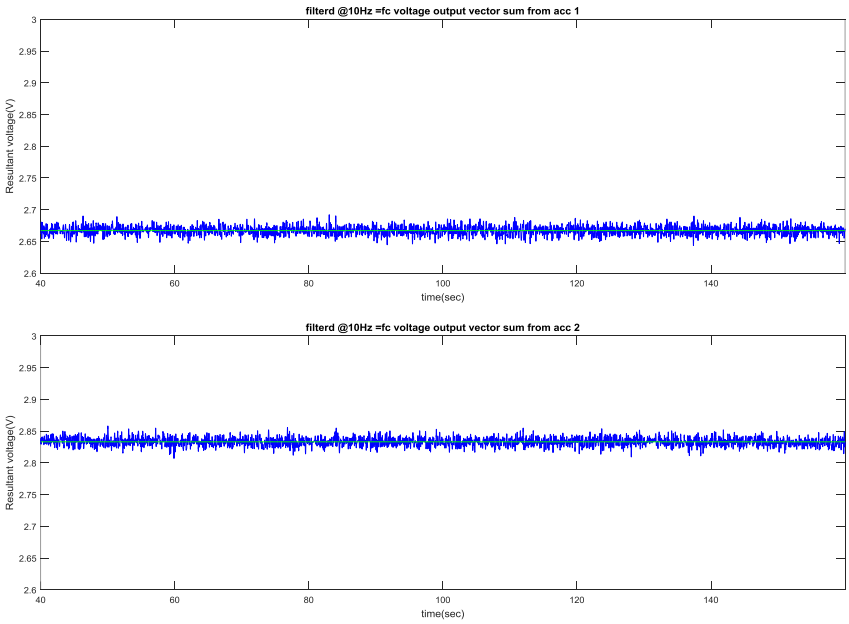

Figure 4.2 Resultant vector plot and the average to calculate 1G voltage assumption Acc1 =2.66V Acc2=2.83V

Table 4.1 Characteristics of the accelerometer in spec sheet according to the supply voltage 3.3V

Supply voltage(V)	Offset voltage(V)	Sensitivity(mV/g)	Resultant voltage from 3 axis(V) under 1G
3.3	1.405	319.4	2.6

4.2 Sample data analysis

The Figure 4.3 shows the raw voltage output with respect to time domain. In the first 3 minutes and extra 20second, the signals came from accelerometers were collected in total 200sec. Because the sample rate was 200Hz, the total length of data, or number of sample is N= 40,000. The data unrelated to the coordinated movement after 200sec was deleted. The rotational parts of the signal after 120 sec was explicit. The accelerometers also send the output voltage of any vibration in the measurement environment. Therefore, the high frequency noise was also contained in the signal due to the current flow and mass of the MEMs accelerometer(mechanical noise in MEMS). The shacking section from 1~2 min was not significantly shown due to these factors in the raw voltage. So the low pass filter (LPF) was considered to remove this high frequency factors.

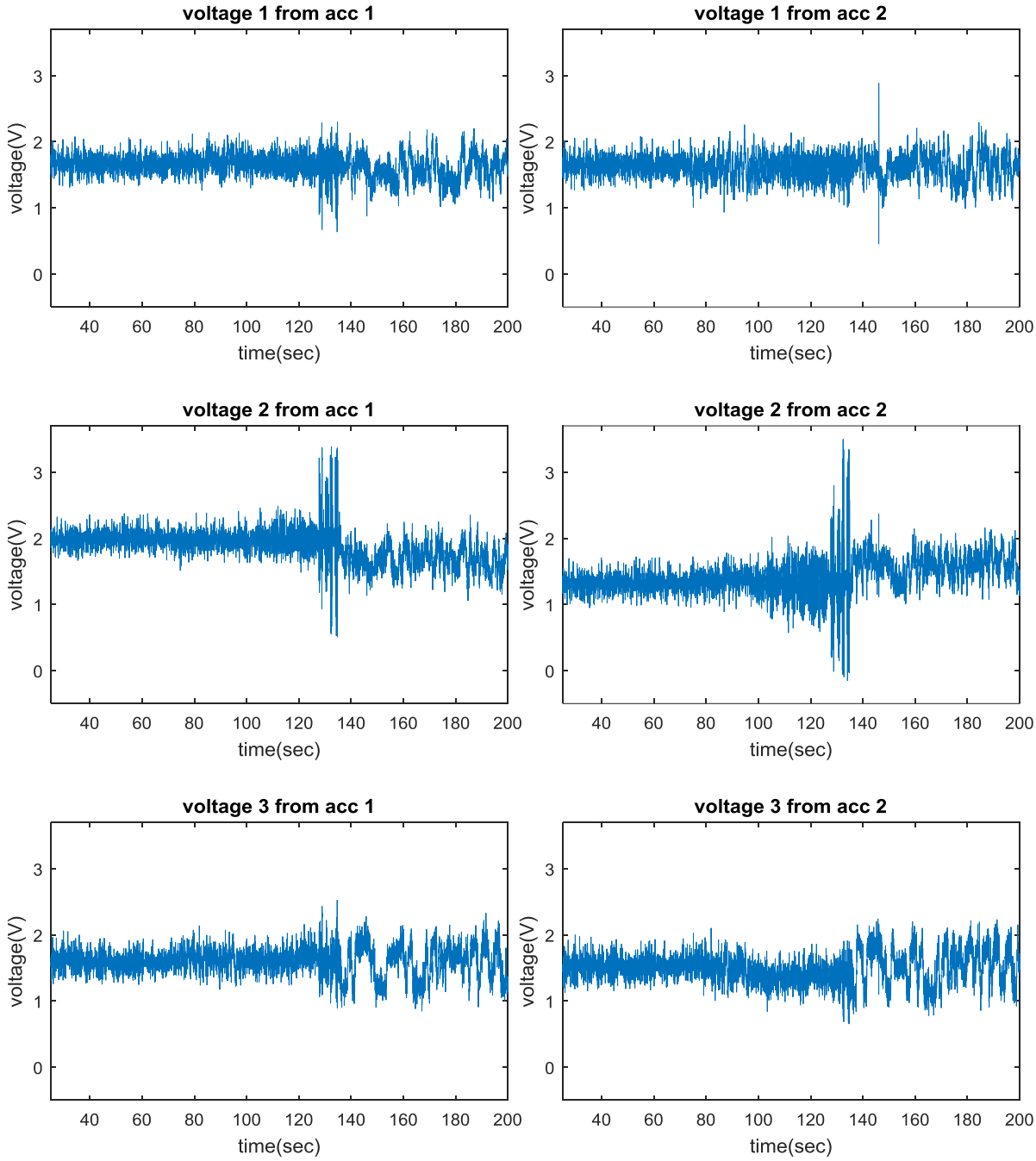

Figure 4.3 Raw data plots from two accelerometers. Left column: acc1, Right column: acc2

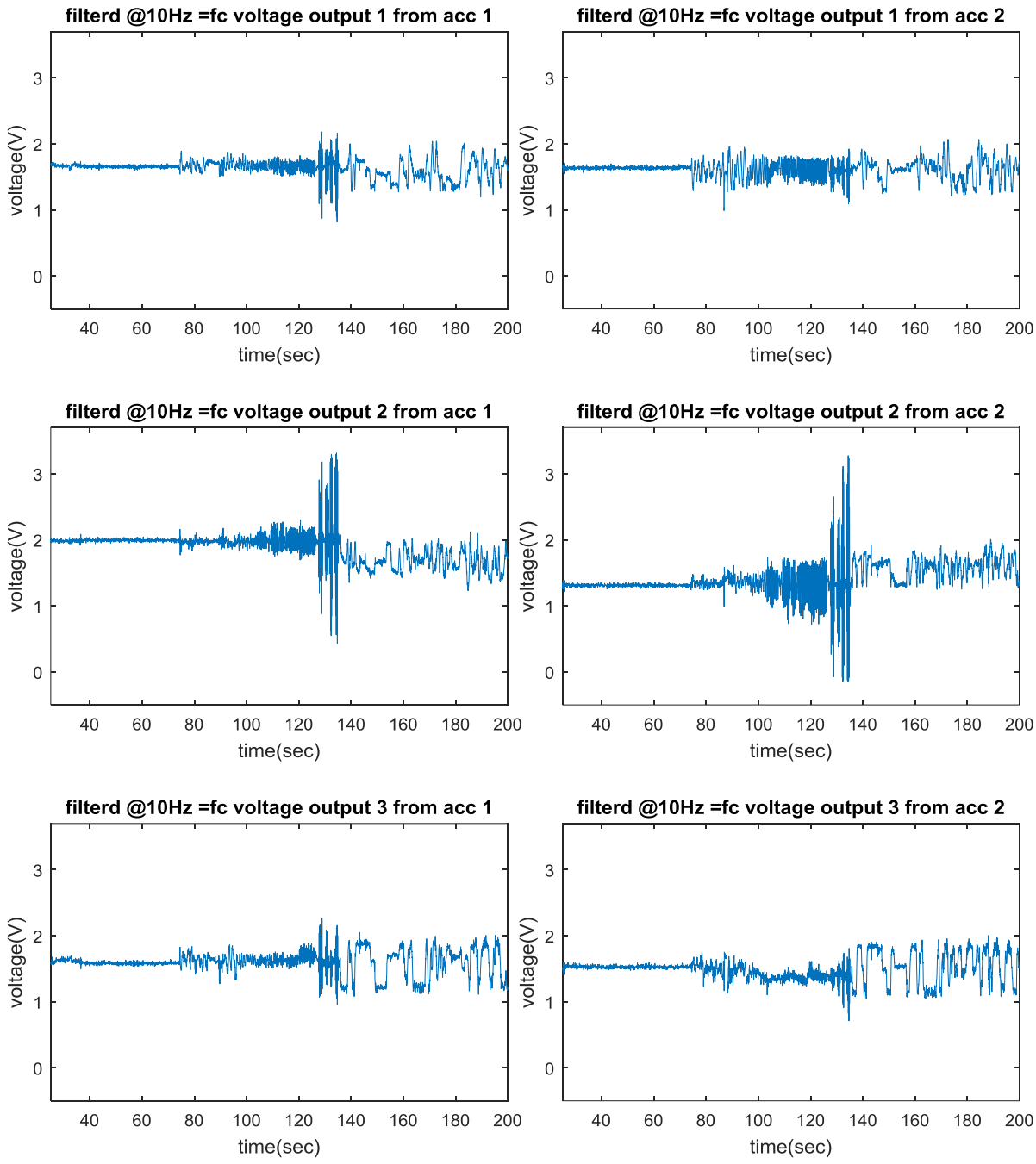

Figure 4.4 Signals acquired from accelerometers and filtered through 10Hz LPF

There are the pre-process before the time frequency analysis. As discussed before, the high frequency factor should be removed to observe the signature movement in Figure 4.2 and Figure 4. Also practically, the baby cannot shaking their limbs higher than 10Hz. Clear movement of shacking was obtained between 80 sec to 120sec compared to the

raw signal plots in Figure 4.3. The first 20-second unstable data is due to the human factor. 6th order Butterworth LPF was designed to get rid of the high frequency component and the result is shown in Figure 4. FRF of the designed filter presented in

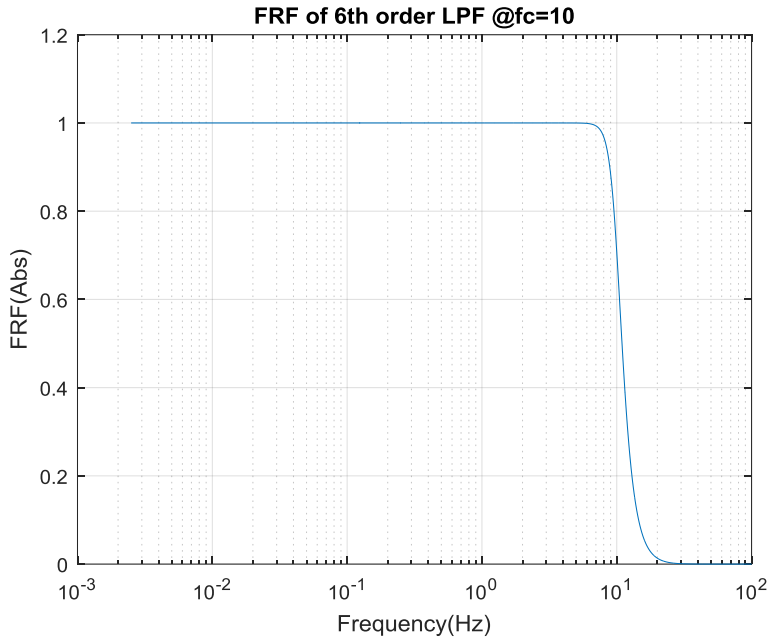

Figure 4.5 FRF of 6th order LPF @ fc=10Hz

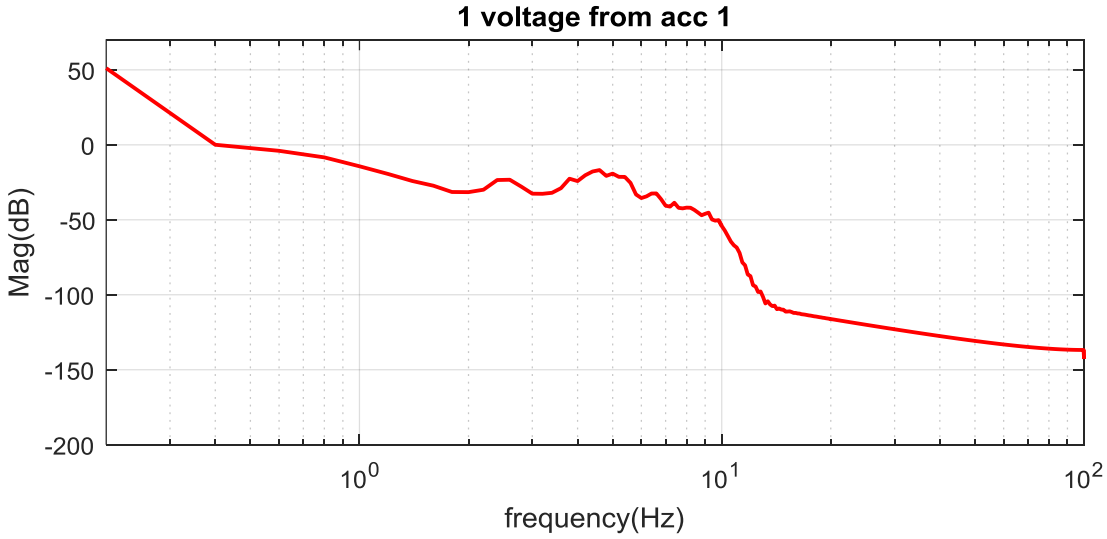

Figure 4.6 Auto spectrum of 1 voltages came from accelerometer 1

To see the filter to remove the high frequency above 10Hz, the FRF for entire time was shown in Figure 4.6. We can see that 6th order Butterworth filter @ 10Hz was applied and the signal shows low amplitude after 10Hz

To find out the relationship between the signals, generated cross spectrum between each signals for entire time range was presented in **Error! Reference source not ound.** . We can see the peak at 4~5Hz that is what we expected. (Low frequency high peak is the DC factor)
The phase difference was not considered in this signal processing, because the coherence does not depend on phase shift.

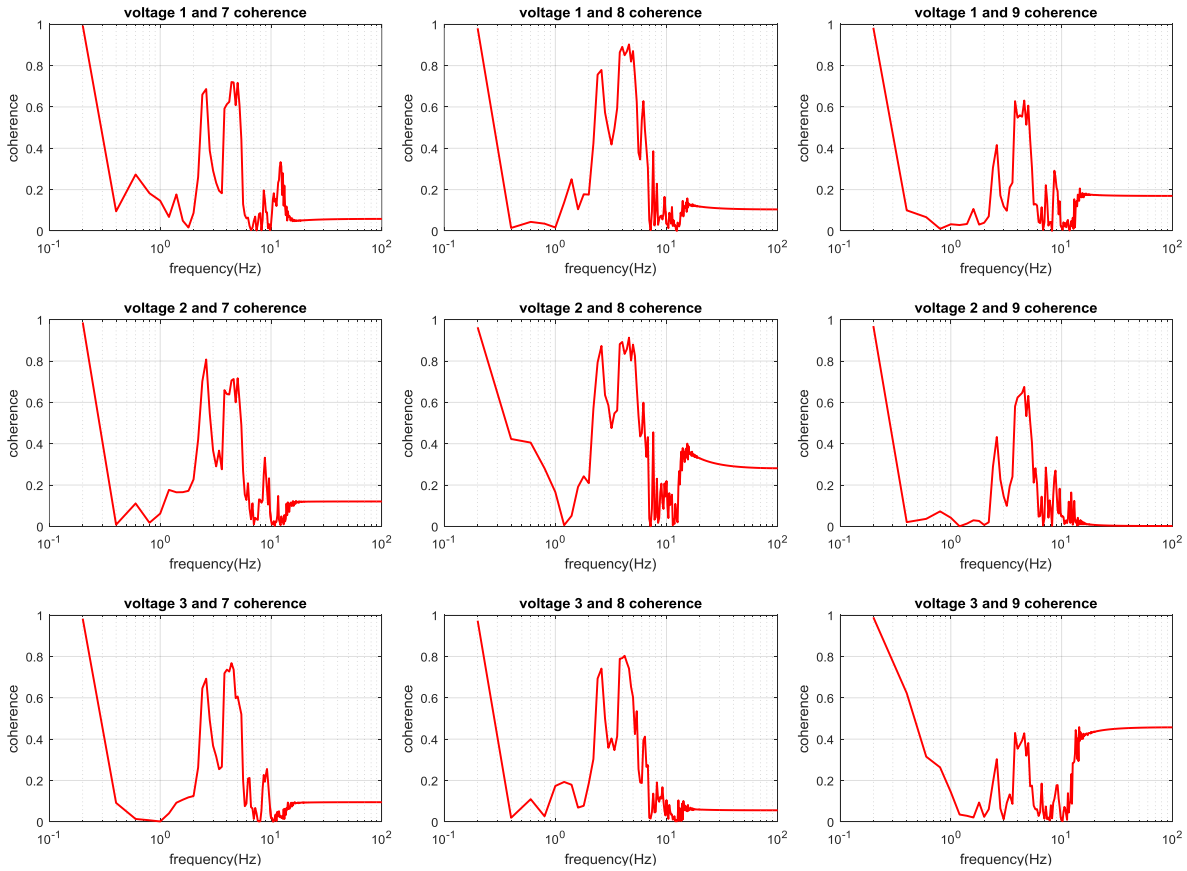

Figure 4.7Coherence of these 9 combinations for entire time range

As discussed in the plots above, in the real data from baby, we use four accelerometers which are composed of 3 axis each. In this chapter, 3 axis outputs from each accelerometer were considered. It means 6 signal outputs and 9 combinations exist to find the correlation between the limbs. The high peaked combinations in these 9 combinations between the accelerometer will be analyzed as time frequency method. In the Figure 4., the high peak above 0.7 was shown in 1-8,2-8,3-8 combinations. The STFT output between these combinations was analyzed in **Error! Reference source ot found.**.

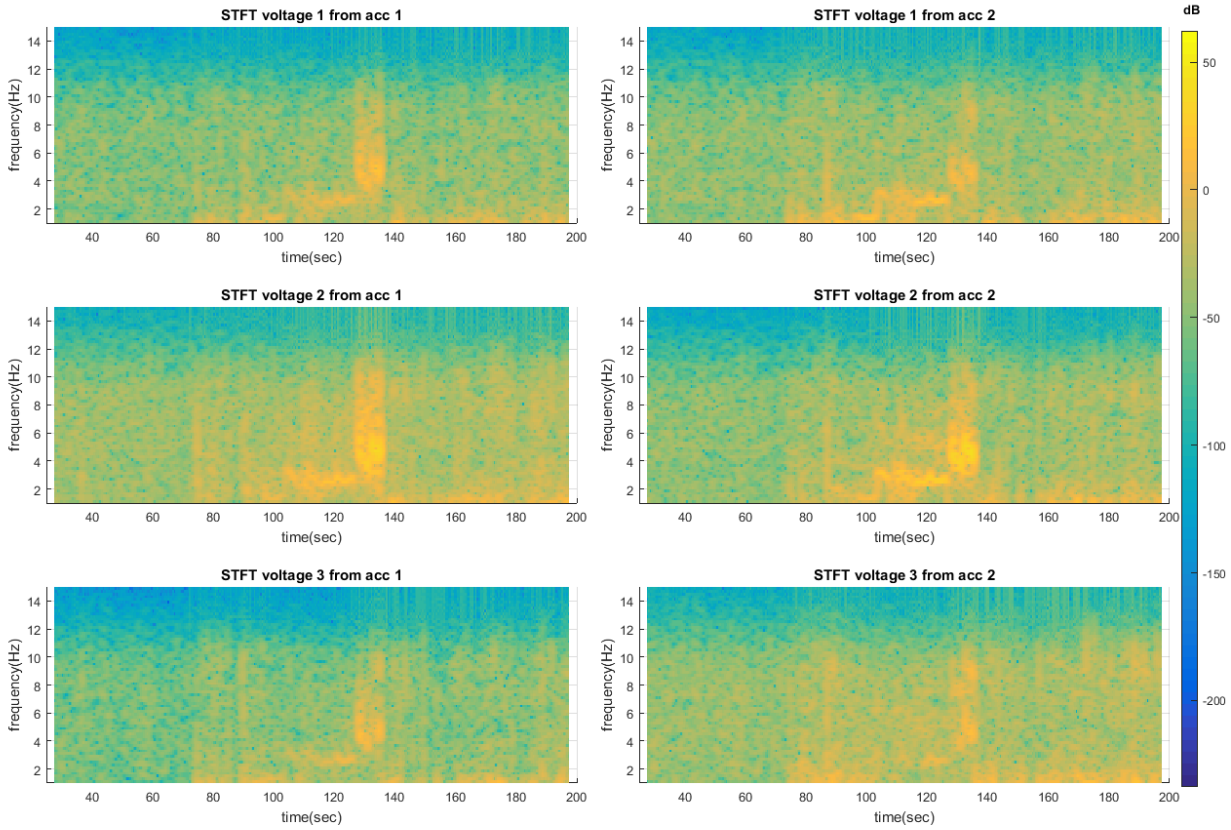

Figure 4.4 Zoomed (from 1Hz to 15Hz) auto spectrum in STFT, time frequency analysis of 6 voltages

The figure shows the Auto spectrum STFT result, if you see the STFT, the auto spectrum with time frequency response shows the filtering affect after 10Hz shows blue and green below 100 db. All nine combinations FRF were shown in this graph. Block size N=1000, total 5sec and averaged recorded time N=10,000 coherence result was also demonstrated. And the increment was every N=100.

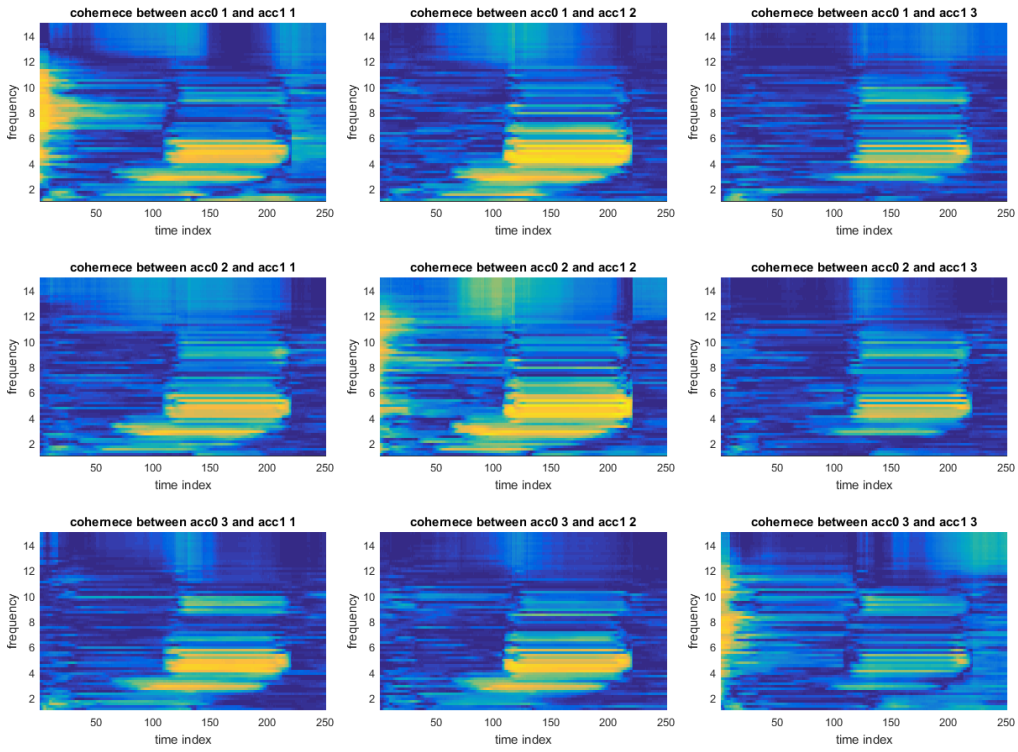

Figure 4.5 Time-frequency Coherence analysis applied Rectangular window 1000, block 10,000 index 100

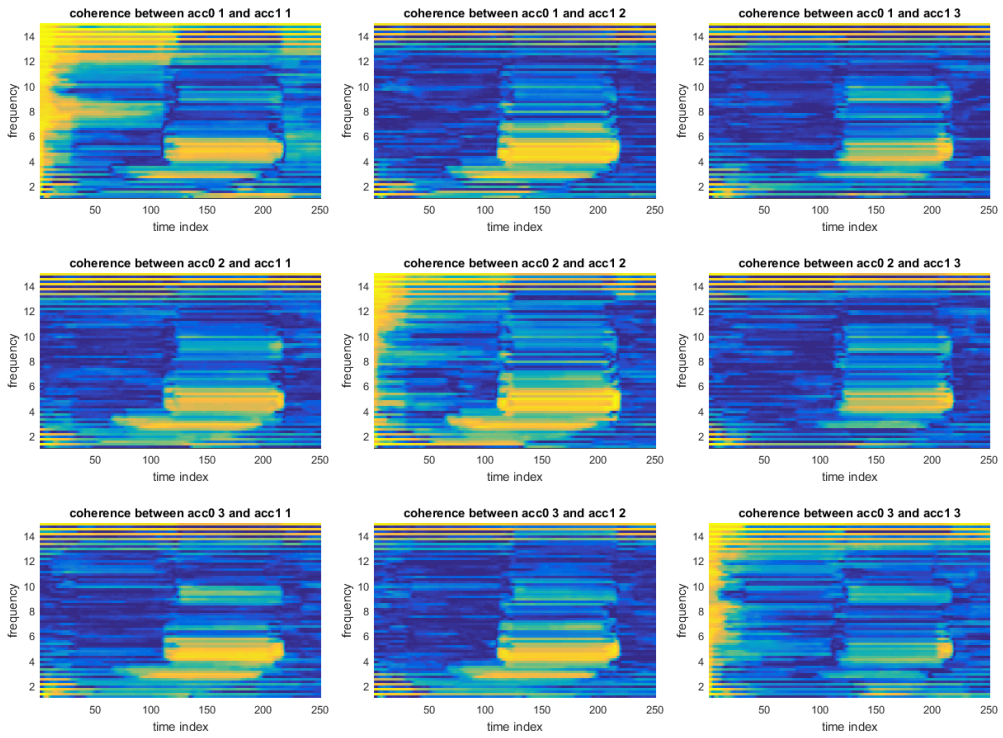

Figure 4.6 Time-frequency Coherence analysis applied triangular window 1000, block 10,000 index 100

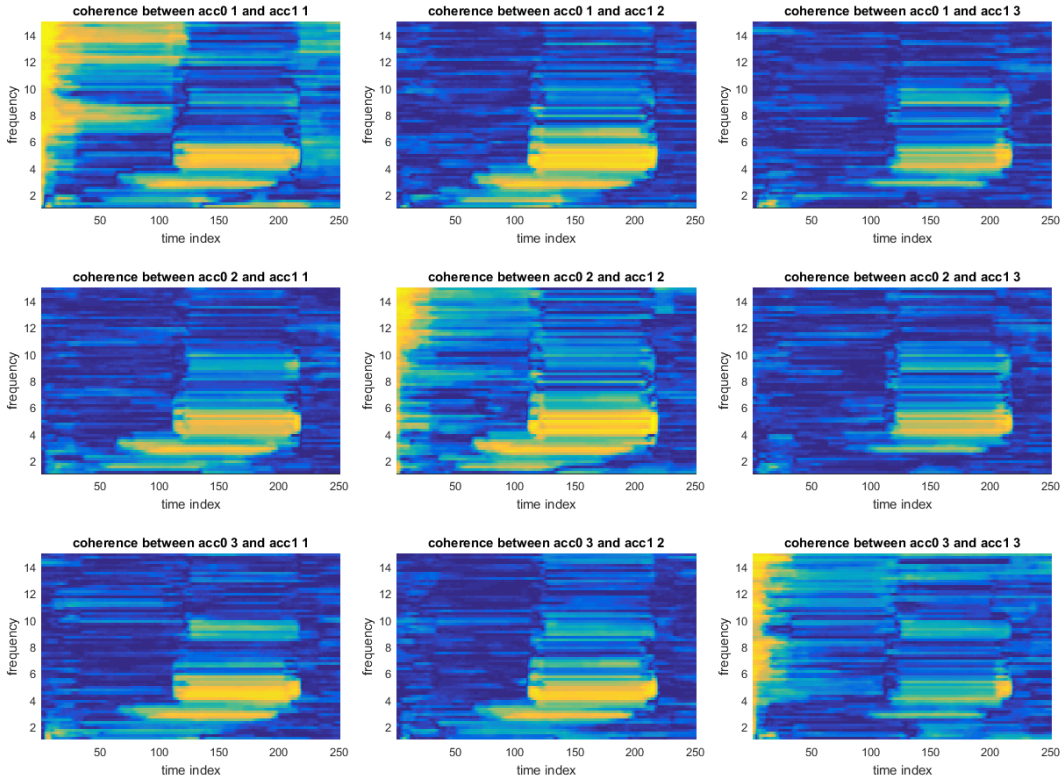

Figure 4.7 Time-frequency Coherence analysis applied Hanning window

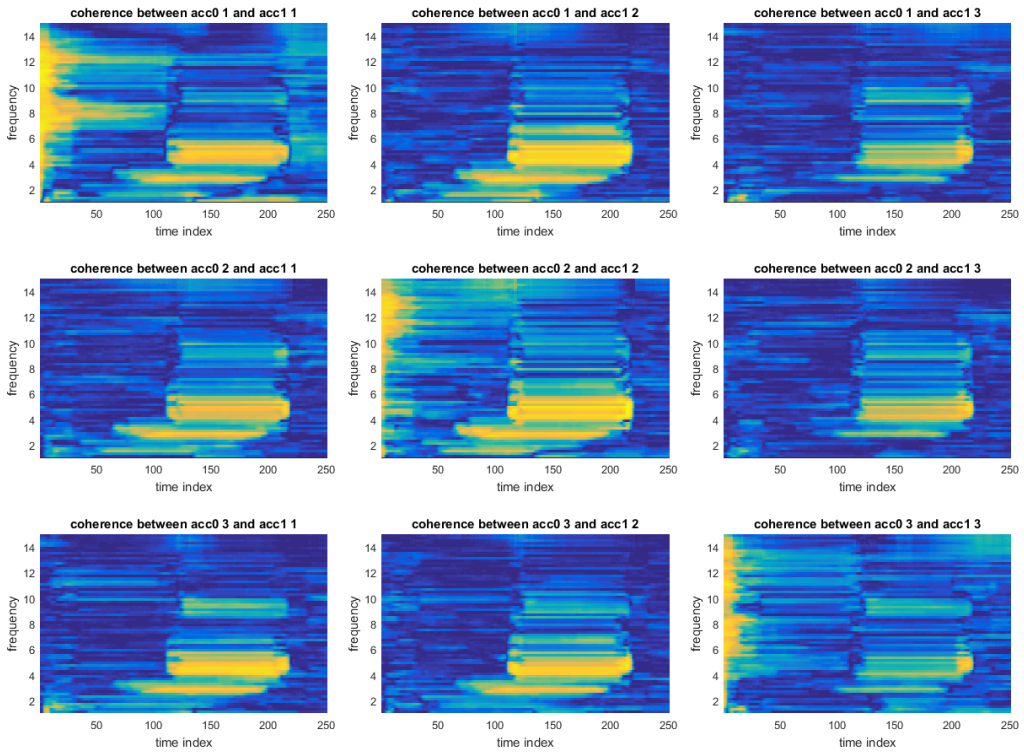

Figure 4.8 Time-frequency Coherence analysis applied Hamming window

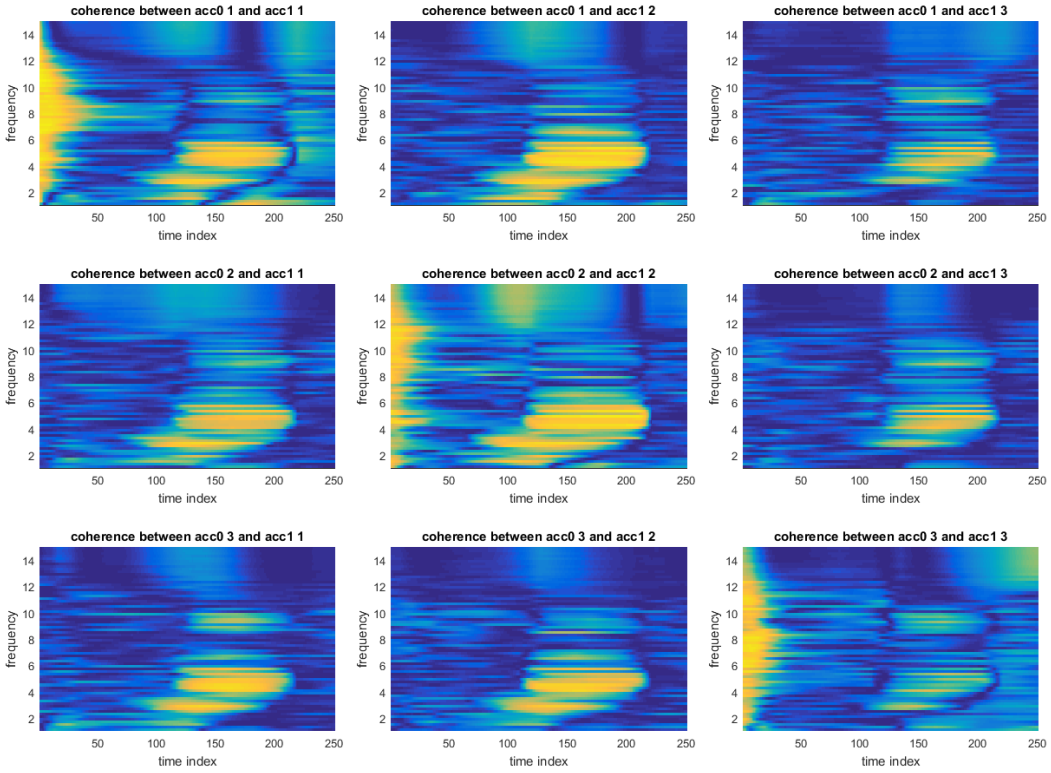

Figure 4.9 Time-frequency Coherence analysis applied weighted average method for 1 to 15Hz frequency graph, rectangular window

4.3 Sample data analysis 2

In the Figure 4.10, from 100 to 200 time index shows the high coherence at certain frequency range, which represents shacking correlated movement from 69sec to 139sec. The bilateral coordination movements between limbs can be displayed by this technique. Therefore, the two other correlated movements were considered to prove the method is correct. Two different correlated movements collected with same sampling frequency and collected in 3 min and 20 sec, N=40000. The first data collected shaking vertically both hand with different amplitude and speed at certain time. The other movement data was collected changing amplitude and the rotating both hands at the same time to simulate the babies correlated movement between the limbs.

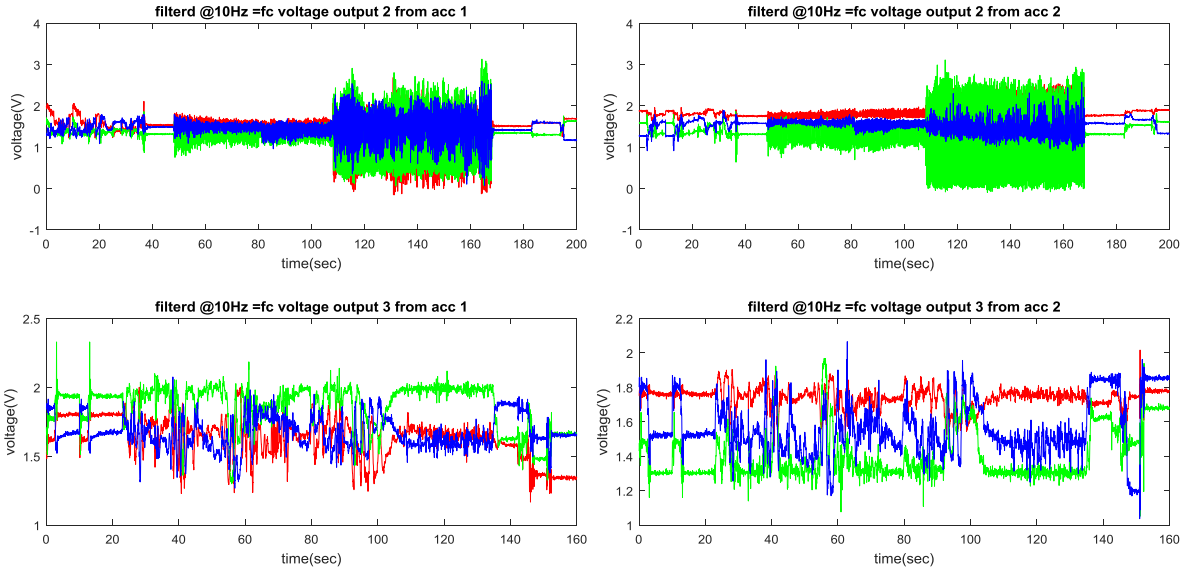

Figure 4.10 Top row: Low frequency High frequency with weighted average from two accelerometers, Bottom row: smooth rotational movement from two upper limbs.

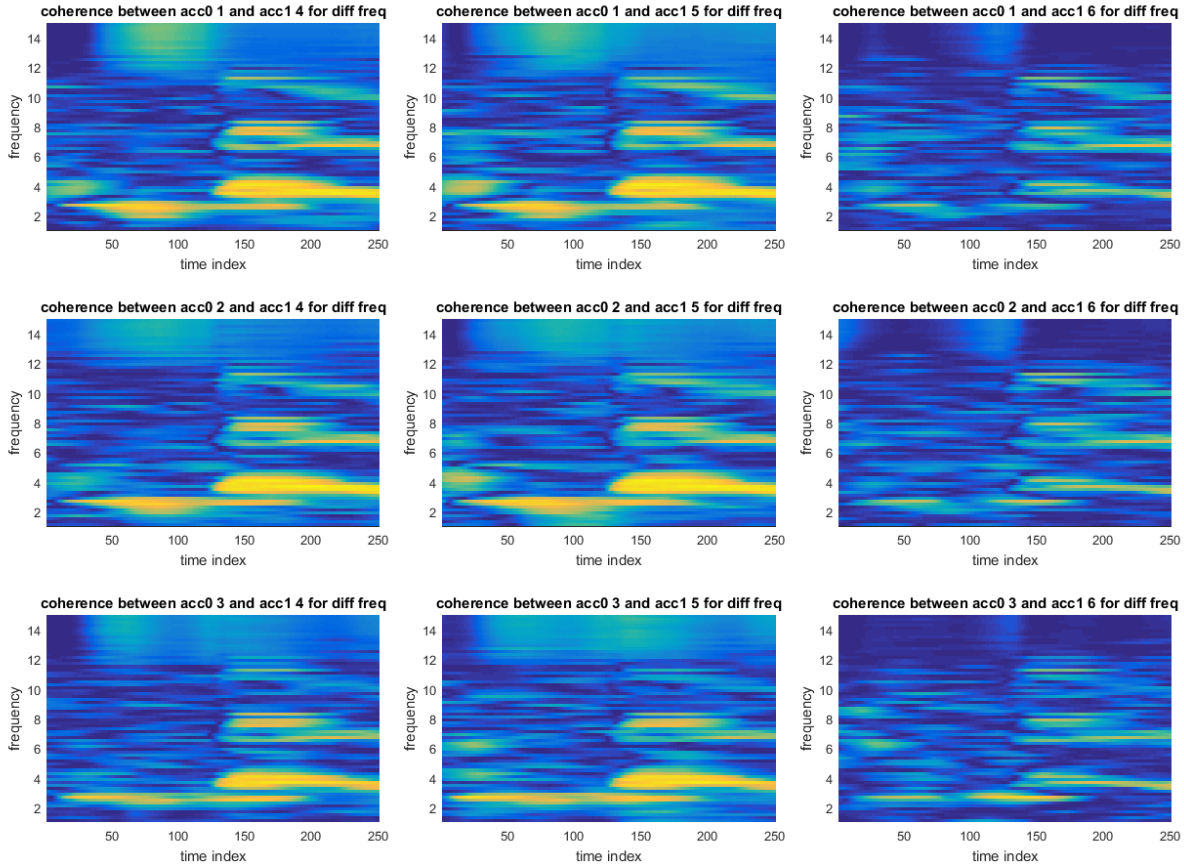

Figure 4.11 Time-frequency Coherence analysis applied weighted average method from 1 to 15Hz frequency graph, rectangular window for Low frequency High frequency shaking movement with respect to time changing

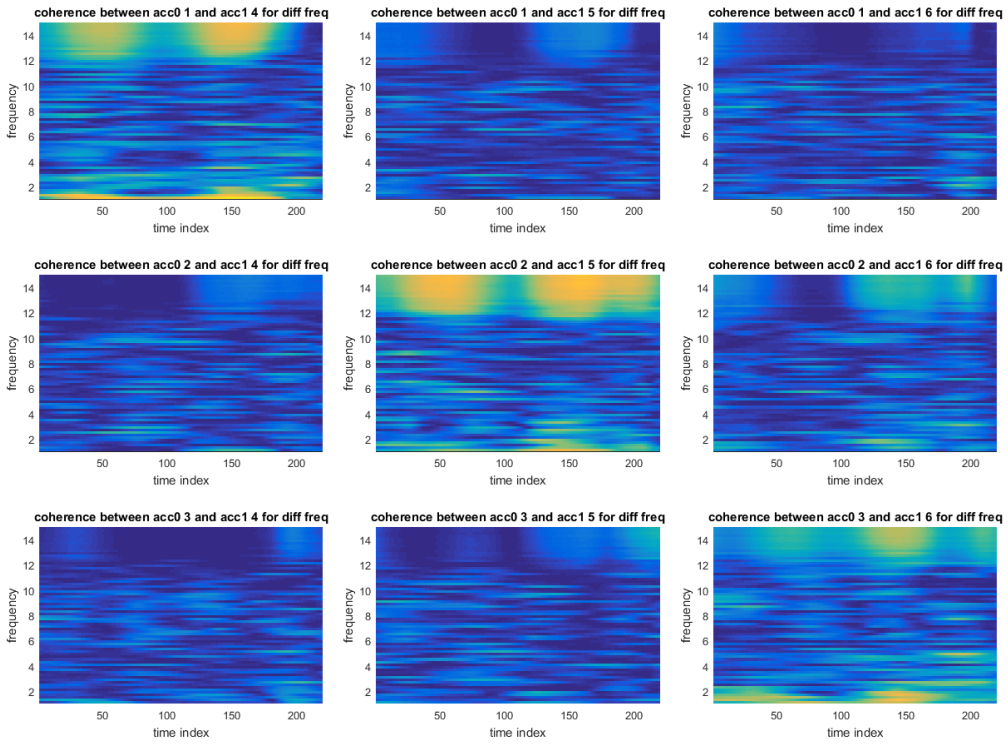

Figure 4.12 Time-frequency Coherence analysis applied weighted average method from 1 to 15Hz frequency graph, rectangular window for gradual rotational movement with weighted average

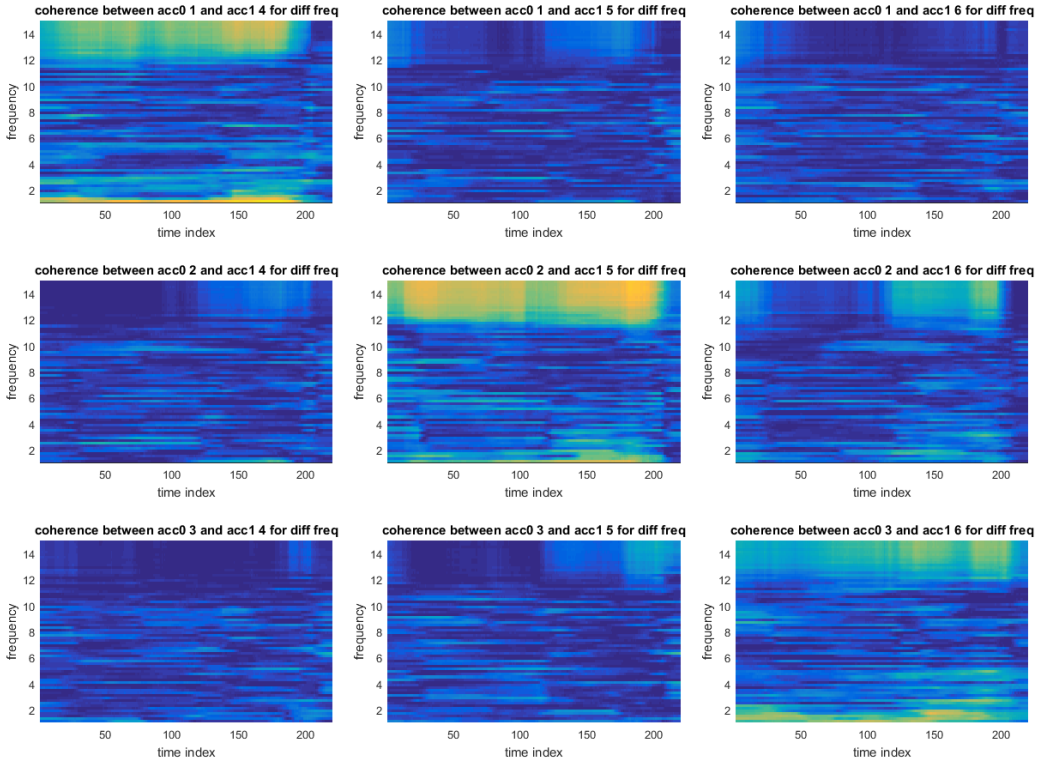

Figure 4.13 Time-frequency Coherence analysis applied weighted average method for 1 to 15Hz frequency graph, rectangular window gradual rotational movement without weighted average

Two extra movements were analyzed to verify the time frequency method. The Figure 4.11 represents the correlated movements of different frequencies. In the first part, the tester shook as low frequency and in the later part shook high frequency. All 9 combinations of the signals shows that a high coherence at low frequency section at the beginning. In the later time, it shows high coherence at high and low frequency at the same time as expected. It can be conclude that the analysis can capture the correlated movement with respect time and frequency.

Secondly, the movement which simulates the baby's upper arms, rotating and shaking arms smoothly and continually was shown in Figure 4.11 and Figure 4.12. All xyz from each accelerometer was well related. The wide range of frequency indicates the high coherence in the wide range of time. Smooth change of correlated motion of the baby can be interpreted quantitatively in these graphs.

In these 3 analysis, the correlated movement represented as the high coherence at the time section and frequency range. However, the rotating movement does not affect coherence a lot. As defined in chapter 2, literature review, the coordinated motions of the infant from 4 to 6months will be changed gradually, we can apply this time frequency analysis technique to measure the correlation as quantitatively.

4.4 Sample data analysis from infant

Finally, to verify the analysis to the real infant data, the researcher collected the signals from the 2-month-old infant with the same hardware setting. The data should be acquired from the infant spontaneously, so the baby creep is equipped in the calm and low light intensity in Figure 4.14Figure 4.14. In the literature review, the infant before 20 weeks shows low alternating kicking movement, which is one of the BCMs. In the assumption, two-month-old infant will show the low correlated movement, therefore, will show the low coherence under 0.7.

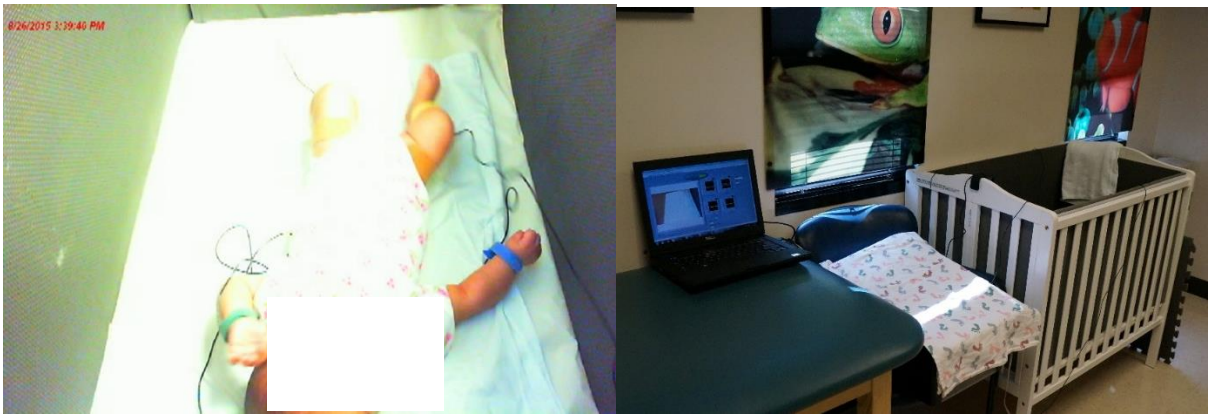

Figure 4.14 two months of an infant with accelerometers and the environmental setting

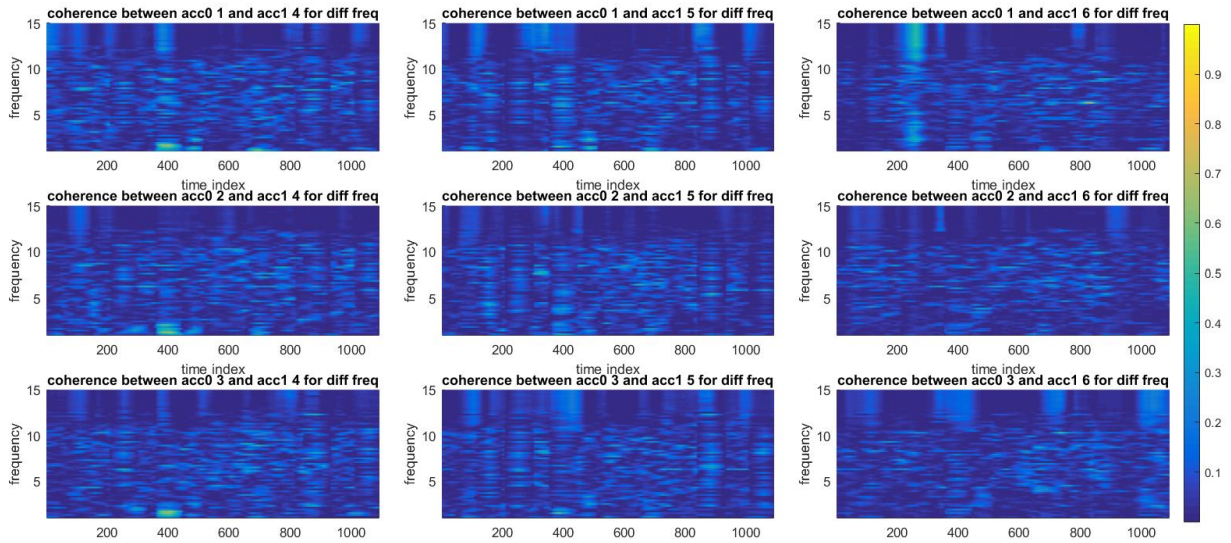

Figure 4.15 3D coherence plot of upper limbs movements under 15Hz.

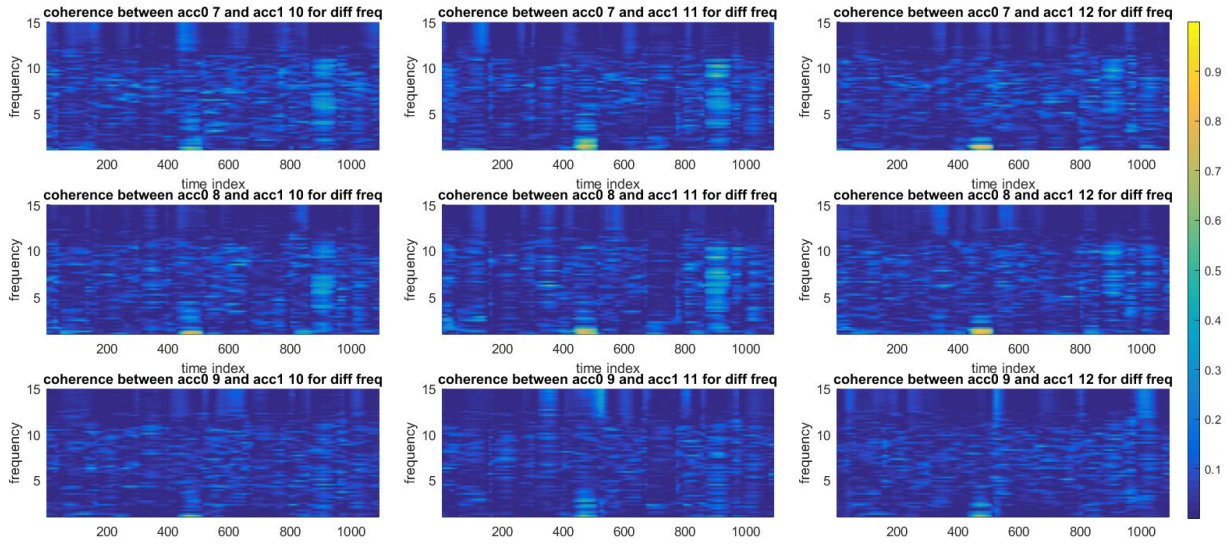

Figure 4.16 3D coherence plot of lower limbs movements under 15Hz.

The 3D coherence plots which evaluated two upper limb and two lower limbs support the assumption of the research. Both plots shows consistently low coherence in the entire time range before 15 Hz because the subject infant cannot show the coordinated movement at this developmental stage. By observing, the shifting patterns according to the infant age can show clearer patterns of normal and abnormal neurological development.

5 Result and Conclusion

As shown in Chapters 3 and 4, the correlated signals were generated by computer and accelerometers. The graphs using time frequency moving average method was shown in the same chapters too. We expected to see the infant movement under the frequency of 10Hz. The researcher could see the high coherence at expected time range and frequency range. The importance of CP diagnosis was discussed in Chapter 2 using the movement of an infant. The infant will show the high correlated movement between the limbs according to the brain development after the FM stage. The bilateral coordinated movement will gradually increase. It can be quantified by the time frequency approach. The researches not only can measure the correlated movements quantitatively, but also can detect the abnormal development of motor disturbance as a result of the brain damage in this early phase. The infant who has brain damage will have low correlated motions. This research can quantify the relationship.

5.1 Analysis of data for CP diagnostics

One of the major CP symptoms, discussed in the literature review in chapter 2, is the motor disturbance which cannot control the limbs correlatively. The average time to diagnose the CP is 18 months with the brain scanning methods. The new signal processing approach can reduce the current time to reach a final diagnosis. With the earlier intervention, the baby can have a better and more independent quality of life. Under 6 months, the baby is supposed to show so called Fidgety Movement: a smooth and continuous movement of each limb. The Fidgety movement will be developed into the intentional and antigravity movement according to the GM's development classification. The researcher assumed that in the normal case, the movement between the limbs is correlated with each other and the brain development will affect the correlated movement. The literature review supported the assumption. Therefore, at

the end of Fidgety movement, after 6 months, if the correlated movement was not observed, it can be considered one of the signs of the brain related issue. To detect this correlation, the accelerometer data was collected and analyzed using the time-frequency method. The coherence in the time and frequency spectrum could demonstrate the correlation in the data collected from the accelerometers which is attached to the arms of the tester. In the future research, the expert can tell whether the infant is experiencing brain damage by collecting the accelerometer data from the infant before the brain scanning method. The standard coherence can be quantified in the future research from the wide survey from new born babies under CP and normal development.

5.2 Reliability of data

Trained experts of GM can detect the baby movement by observation and it is related to the correlation of the movements of the infant. As shown in chapter 4, two correlated signals in the low frequency and the high frequency were generated in order at specific time period. The calculated coherence was near 1 (perfectly correlated) at these specific time range and frequency accordingly. The time frequency method was validated as researcher designed. In addition, the final data analysis was done and showed that the coherence was low because of the age of the infant, which was younger than 6 months. The specific coherence can be attained by future study.

5.3 Future work

This analysis can be applied to the other diseases or syndromes which demonstrate bilateral coordination disturbances. Also the severity classification can be measured by this method. As discussed in the previous part of the chapter, statistical data needs to be collected to set a specific range in order to decide the normal and abnormal bilateral movement. It is necessary that the future research target broad and expanded data from infants under CP or normal development. Thus, the coherence threshold to diagnose CP will be studied in the future research. Finally, the research

defined the relationship of the limb's movement quantitatively, so the method can be applied to the other diseases or syndromes which affect motor disturbances.

One of the possible applications is to estimate the severity about Parkinson 's disease. One of the major symptoms in Parkinson's disease is the motor disturbance and the difficulty controlling all limbs correlatively. The Parkinson's disease does not have a perfect cure at this point. Instead of that, the early intervention is recommended for the better quality of life and independent life. This new signal processing approach can be used to measure the progress of the disease. Also, the massive research for the statistical analysis is needed to acquire the appropriate standards. Quantitative analysis based on the movement can provide the blue print of the progression of the stages of the disease.

Currently, the data acquisition system is made of four xyz axis accelerometers with wire. The signal was collected through DAQ acquisition system through LabVIEW. This system is a prototype to test the data analysis but there are possible improvements in the current hardware system. First of all, the system can be upgraded from wired to the wireless by implementing a new microcontroller which supports Bluetooth function. Secondly, researcher used NI-9107 12bit ADC, and it was good enough hardware to collect the signal, but there is possibility to increase the resolution of LSB (least significant bit) by upgrading the ADC. Also in the current system, the changing of the angle was not actively considered to calculate the correlation, but the embedded gyroscope can provide a user better chance to analyze the data in a different perspective point of view. Lastly, the testing device was not easily assessable. The recent development of wearable devices which includes accelerometers and gyroscope can provide easy access to anyone. In other words, with wearable devices such as, apple-watch, android smart watch and fitness wearable devices, this research can provide a tool for users who need continuous self-observations suffering from Parkinson syndrome or CP syndrome. The patients who have these diseases need to practice activities that enhance the functionality of the nervous system. These wearable devices

can easily collect signals and observe the motor disturbance over the time by the time-frequency analysis technique.

In this research, the researcher tested time-frequency averaging method to quantify the bilateral coordinate movements. Therefore, the resulted plots showed as expected by representing high coherence at targeted time and frequency. The method can help the people who need to monitor the correlated motions according to the time changes.

6 Reference

6.1 Literature review reference

[1] P. Stern Law Group, "cerebralpalsy.org/about-cerebral-palsy/definition/," [Online]. [Accessed 5 11 2015].

[2] "Cerebral Palsy: Hope Through Research," National Institute of Neurological Disorders and stroke, 2 July 2015. [Online]. Available: http://www.ninds.nih.gov/disorders/cerebral_palsy/detail_cerebral_palsy.htm. [Accessed 5 11 2015].

[3] "Important Milestones: Your Child at One Year," Center of Disease control and prevention, 27 March 2014. [Online]. Available: http://www.cdc.gov/ncbddd/actearly/milestones/milestones-1yr.html. [Accessed 5 11 2015].

[4] "Economic costs associated with mental retardation, cerebral palsy, hearing loss, and vision impairment," *Morbidity and Mortality Weekly Report (MMWR),* vol. 9, pp. 53-57, 2003.

[5] Einspieler C1, Prechtl HF., "Prechtl's assessment of general movements: a diagnostic tool for the functional assessment of the young nervous system.," *Mental Retardiation and development disablities,* vol. 11, pp. 61-67, 2005.

[6] Lars Adde, Jorunn L Helbostad, Alexander Refsum Jensenius, Gunnar Taraldsen and Ragnhild Støen, "Using computer-based video analysis in the study of fidgety movements.," Vols. epartment of Clinical Services, Physiotherapy section, St. Olav University Hospital, Trondheim, Norway. lars.adde@ntnu.no, no. Department of Clinical Services, Physiotherapy section, St. Olav University Hospital, Trondheim, Norway. lars.adde@ntnu.no, 2009; 85(9) DOI: 10.1016/j.earlhumdev.2009.05.00.

[7] Edward Taub, Sharon Landesman Ramey, Stephanie DeLuca, Karen Echols, "Efficacy of Constraint-Induced Movement Therapy for Children With Cerebral Palsy With Asymmetric Motor Impairment," *American Academy of Pediatrics,* vol. 113, no. 2, pp. 305-312, February 2004.

[8] " Korean Cerebral Palsy information center," kiccp, 2000-2015. [Online]. Available: http://www.kiccp.org/index.php?mm_code=76&PHPSESSID=559275d8febd7210da3d9f00489073ed. [Accessed 11 5 2015].

[9] H.-A. M, "Early Diagnosis and Early Intervention in Cerebral Palsy," *frontier in neurology,* vol. 5, p. 185, 2014.

[10] "CerebralPalsy.org," Stern Law Group, PLLC, [Online]. Available: http://cerebralpalsy.org/about-cerebral-palsy/diagnosis/12-step-process/. [Accessed 7 11 2015].

[11] Christa Einspieler, Peter B. Marschik, and Heinz F.R. Prechtl, "human motor behavior Prenatal Origin and Early Postnatal Development," *Zeitschrift für Psychologie / Journal of Psychology,* vol. Vol. 216(3):, p. 148–154, 2008.

[12] D. C. Einspieler, "General Movement Trust," Institute of Physiology, Medical University Graz, [Online]. Available: http://general-movements-trust.info/. [Accessed 5 11 2015].

[13] Lars Adde, Jorunn L. Helbostad, Alexander Refsum Jensenius, Gunnar Taraldsen, Ragnhild Støen, "Early prediction of cerebral palsy by computer-based video analysis of general movements: a feasibility study," *Developmental Medicine & Child Neurology,* vol. 52, no. 8 , p. 773–778, August 2010.

[14] P. Rahmanpour, "features for movement based prediction for cerebral palsy," *Master of Science in Engineering Cybernetics,* June 2009.

6.2 Accelerometer spec sheet

http://www.farnell.com/datasheets/1789311.pdf

7 Appendix

A LabVIEW code

B Matlab code

```
%%3.1 figures

fs=50;
Ts=1/fs;
t=[Ts:Ts:2];
N=length(t);
y=sin(2*pi*t);
yf=fft(y);
Fr=fs/N;
F=Fr*[0:N-1];
figure
subplot(4,1,1)
scatter(t,y)
xlabel('time(sec)')
ylabel('amplitude')
title('sin(2*pi*t) , T=1 sec and fs=50Hz')
subplot(4,1,2)
plot(F,real(yf));
xlabel('frequency(Hz)')
ylabel('amplitude')
title('Real part of FFT')
subplot(4,1,3)
plot(F,imag(yf));
```

```
xlabel('frequency(Hz)')
ylabel('amplitude')
title('Imaginary part of FFT')
subplot(4,1,4)
plot(F,abs(yf));
xlabel('frequency(Hz)')
ylabel('amplitude')
title('Modulus of FFT')



%%chapter 3.2
fs=100;
Ts=1/fs;
N=1024;
t=Ts*[0:N-1];
Fr=fs/N;
%%white noise
x1=randn(1,N);
%%sinosoidal 1Hz
x2=cos(2*pi*t);

[R1,k] = xcorr(x1,x1);
[R2,k] = xcorr(x2,x2);

tau=Ts*k;

figure
subplot(2,2,1)
plot(t,x1)
subplot(2,2,2)
plot(tau,R1)
subplot(2,2,3)
plot(t,x2)
subplot(2,2,4)
plot(tau,R2)

%%chapter 3.3
fs=100;
N=2^10;
Ts=1/fs;
t=Ts*[0:N-1];
%stationary signal
y1=cos(20*pi*t);
%non-stationary signal
y2=y1;
whiteN=randn(1,N);
for i=1:round(N/2)
    y2(i)=whiteN(i);
end


figure
subplot(2,1,1)
plot(t,y1)
```

```
xlabel('time(sec)')
ylabel('amplitude')
title('stationary data of sinosoidal of 10Hz')
subplot(2,1,2)
plot(t,y2)
xlabel('time(sec)')
title('non- stationary data white noise and sinosoidal of 10Hz')
ylabel('amplitude')


nfft = 2^8;
wndo = nfft;
ovlp = nfft/2;

[Pxx1,FR] = pwelch(y1,wndo,ovlp,nfft,fs);
[Pxx2,FR] = pwelch(y2,wndo,ovlp,nfft,fs);

Pxx1=Pxx1*fs/2;
Pxx2=Pxx2*fs/2;


figure
subplot(2,1,1)
semilogx(FR,20*log10(abs(Pxx1)),'Linewidth',1.5);
grid on
xlabel('frequency(Hz)')
ylabel('magnitude(dB)')
subplot(2,1,2)
semilogx(FR,20*log10(abs(Pxx2)),'Linewidth',1.5);
grid on
xlabel('frequency(Hz)')
ylabel('magnitude(dB)')

% stationay analysis
u=y1;
y=y2;

[Suu,fr] = cpsd(u,u,wndo,ovlp,nfft,fs);
%[Snn,fr] = cpsd(n,n,wndo,ovlp,nfft,fs);
[Syy,fr] = cpsd(y,y,wndo,ovlp,nfft,fs);
%[Sun,fr] = cpsd(u,n,wndo,ovlp,nfft,fs);
[Syu,fr] = cpsd(y,u,wndo,ovlp,nfft,fs);
[Suy,fr] = cpsd(u,y,wndo,ovlp,nfft,fs);
%[Syn,fr] = cpsd(y,n,wndo,ovlp,nfft,fs);

Suu=Suu*fs/2;
Syu=Syu*fs/2;
Suy=Suy*fs/2;
Syy=Syy*fs/2;

H1 = Syu ./ Suu;
H2 = Syy ./ Suy;

%H = squeeze(freqresp(plant,2*pi*fr));
%gamma1 = (Syu .* Suy) ./ (Suu .* Syy);
```

```
%gamma2 = mscohere(u,y,wndo,ovlp,nfft,fs);
figure
semilogx(fr,20*log(abs(H1)));
grid on
xlabel('frequency(Hz)')
ylabel('magnitude(dB)')


%%% non-stationary analysis
nfft = 2^7;
wndo = nfft;
ovlp = nfft/2;

%part 1
u=y1(1:2^9);
y=y2(1:2^9);

[Suu,fr] = cpsd(u,u,wndo,ovlp,nfft,fs);
%[Snn,fr] = cpsd(n,n,wndo,ovlp,nfft,fs);
[Syy,fr] = cpsd(y,y,wndo,ovlp,nfft,fs);
%[Sun,fr] = cpsd(u,n,wndo,ovlp,nfft,fs);
[Syu,fr] = cpsd(y,u,wndo,ovlp,nfft,fs);
[Suy,fr] = cpsd(u,y,wndo,ovlp,nfft,fs);
%[Syn,fr] = cpsd(y,n,wndo,ovlp,nfft,fs);

Suu=Suu*fs/2;
Syu=Syu*fs/2;
Suy=Suy*fs/2;
Syy=Syy*fs/2;

H11 = Syu ./ Suu;
H2 = Syy ./ Suy;

figure
semilogx(fr,20*log(abs(H1)));
grid on
xlabel('frequency(Hz)')
ylabel('magnitude(dB)')

%part 2
u=y1(2^9+1:2^10);
y=y2(2^9+1:2^10);

[Suu,fr] = cpsd(u,u,wndo,ovlp,nfft,fs);
%[Snn,fr] = cpsd(n,n,wndo,ovlp,nfft,fs);
[Syy,fr] = cpsd(y,y,wndo,ovlp,nfft,fs);
%[Sun,fr] = cpsd(u,n,wndo,ovlp,nfft,fs);
[Syu,fr] = cpsd(y,u,wndo,ovlp,nfft,fs);
[Suy,fr] = cpsd(u,y,wndo,ovlp,nfft,fs);
%[Syn,fr] = cpsd(y,n,wndo,ovlp,nfft,fs);

Suu=Suu*fs/2;
Syu=Syu*fs/2;
Suy=Suy*fs/2;
Syy=Syy*fs/2;
```

```
H12 = Syu ./ Suu;
H2 = Syy ./ Suy;

figure
subplot(2,1,1)
semilogx(fr,20*log(abs(H11)));
grid on
xlabel('frequency(Hz)')
ylabel('magnitude(dB)')
subplot(2,1,2)
semilogx(fr,20*log(abs(H12)));
grid on
xlabel('frequency(Hz)')
ylabel('magnitude(dB)')
```

```
%%%chapter 3.6 and 3.7
figure
subplot(2,1,1)
semilogx(FR,10*log10(abs(Pxx1*(fs/2))),'r');
grid on
xlabel('frequency(Hz)')
ylabel('FRF of stationary data of sinosoidal of 10Hz(dB)')

subplot(2,1,2)
semilogx(FR,10*log10(abs(Pxx2*(fs/2))),'r')
xlabel('frequency(Hz)')
grid on
ylabel('FRF of non-stationary data of white noise and sinosoidal of 10Hz ')

figure
[S,F,T] = spectrogram(x3,wndo,ovlp,fr,fs);
contour(T,F,S)

%%half half
nfft = N/8;
wndo = nfft;
ovlp = nfft/2;
x3_h1=zeros(1,2^11);
x3_h2=x3_h1;

x3_h1=y2(1:2^11);
x3_h2=y2((2^11+1):2^12);

[Pxxh1,FR] = pwelch(x3_h1,wndo,ovlp,nfft,fs);
[Pxxh2,FR] = pwelch(x3_h2,wndo,ovlp,nfft,fs);
```

```
figure
subplot(1,2,1)
semilogx(FR,10*log10(abs(Pxxh1*(fs/2))),'r')
xlabel('frequency(Hz)')
ylabel('dB')
grid on
title('FRF of non stationary data only for white noise time section')

subplot(1,2,2)
semilogx(FR,10*log10(abs(Pxxh2*(fs/2))),'r')
xlabel('frequency(Hz)')
ylabel('dB')
grid on
title('FRF of non stationary data only for sin wave time section')
```

```
%%chapter 3.7
fs=400;
Ts=1/fs;
N=2^12;
Fr=fs/N;
t=Ts*[0:N-1];
fr=Fr*[0:N-1];

f1=5;
f2=10;
f3=40;

x0=randn(1,N);
x0=x0/sqrt(N)
x1=cos(2*pi*t*f1);
x2=cos(2*pi*t*f2);
x3=cos(2*pi*t*f3);

x=x0+x1+x2+x3;

nfft = 2^10;
wndo = nfft;
ovlp = nfft/2;


%%x1=x1/sqrt(N); %normalized
figure
subplot(5,1,1)
plot(t(1:100),x0(1:100))
title('White noise')
subplot(5,1,2)
plot(t(1:100),x1(1:100))
title('cosine @5Hz')
```

```
subplot(5,1,3)
plot(t(1:100),x2(1:100))
title('cosine @10Hz')
subplot(5,1,4)
plot(t(1:100),x3(1:100))
title('cosine @20Hz')
subplot(5,1,5)
plot(t(1:100),x(1:100),'r')
xlabel('time(sec)')
ylabel('Amplitude')
title('5Hz, 10Hz,20Hz and whiteNoise')

nfft = 2^10;
wndo = nfft;
ovlp = nfft/2;
u=x;
y=y;

[Suu,fr] = cpsd(x,x,wndo,ovlp,nfft,fs);
Suu=Suu*fs/2;

figure
semilogx(fr,20*log10(abs(Suu)),'r','LineWidth',1.5);
xlabel('frequency(Hz)')
ylabel('Mag(dB)')
title('Frequency response of signal @5Hz,@10Hz,4Hz and noise')
grid on

%design filter
[num,den]=butter(8,0.2); %cutoff freqeuncy as 200*0.1=40Hz

y0=filter(num,den,x0); %pass through filter white noise
y1=filter(num,den,x1); %pass through filter 5Hz
y2=filter(num,den,x2); %pass through filter 10Hz
y3=filter(num,den,x3); %pass through filter 40Hz

y=zeros(1,N);
%combine all these output as one plot with different time section
y(1:2^10)=y0(1:2^10);
y(2^10+1:2^11)=y1(2^10+1:2^11);
y(2^11+1:2^10*3)=y2(2^11+1:2^10*3);
y(2^10*3+1:2^12)=y3(2^10*3+1:2^12);


%%plot u and y

figure
subplot(2,1,1)
plot(t,x)
xlabel('time(sec)')
ylabel('input')
title('sinosoidal combined input @5, 10, 40Hz and white noise')
subplot(2,1,2)
plot(t,y)
title('ouput pass through LPF @0.1*200Hz at different time section ')
```

```
xlabel('time(sec)')
ylabel('output')

u=x;
nfft = 2^8;
wndo = nfft;
ovlp = nfft/2;

[Suu,fr] = cpsd(u,u,wndo,ovlp,nfft,fs);
%[Snn,fr] = cpsd(n,n,wndo,ovlp,nfft,fs);
[Syy,fr] = cpsd(y,y,wndo,ovlp,nfft,fs);
%[Sun,fr] = cpsd(u,n,wndo,ovlp,nfft,fs);
[Syu,fr] = cpsd(y,u,wndo,ovlp,nfft,fs);
[Suy,fr] = cpsd(u,y,wndo,ovlp,nfft,fs);
%[Syn,fr] = cpsd(y,n,wndo,ovlp,nfft,fs);

Suu=Suu*fs/2;
Syu=Syu*fs/2;
Suy=Suy*fs/2;
Syy=Syy*fs/2;

H1 = Syu ./ Suu;
H2 = Syy ./ Suy;
%H = squeeze(freqresp(plant,2*pi*fr));
gamma1 = (Syu .* Suy) ./ (Suu .* Syy);
gamma2 = mscohere(u,y,wndo,ovlp,nfft,fs);
figure
semilogx(fr,20*log(abs(H1)));



figure
semilogx(fr,gamma1,'r','Linewidth',1.5);
grid on
xlabel('frequency(Hz)')
ylabel('coherence')
title('coherence of output')

nfft = 2^8;
wndo = 2^8;
ovlp = wndo/2;
gamma =zeros(4,129);

[Su,Fu,Tu,Pu]=spectrogram(u,wndo,ovlp,nfft,fs);
[Sy,Fy,Ty,Py]=spectrogram(y,wndo,ovlp,nfft,fs);

surf(Ty,Fy,10*log10(abs(Py)),'EdgeColor','none');

nfft = 2^8;
wndo = 2^8;
ovlp = wndo/2;
gamma=zeros(8,nfft/2+1);

for i=1:8
```

```
    strt= (i-1)* 2^9+1;
    ed=i*2^9;
    [gamma(i,:),f]=mscohere(u(strt:ed),y(strt:ed),wndo,ovlp,nfft,fs);
end
figure
tg=[0:8-1]*N*Ts/7;
surf(tg,f,gamma','EdgeColor','none')
colorbar


%%%%chapter 3.6 figure
fs=100;
N=2^12;
Ts=1/fs;
t=Ts*[0:N-1];
%signal input
x1=randn(1,N);
sample=x1;

[num,den]=butter(6,0.25);
y1=filter(num,den,x1);

figure
subplot(2,1,1)
plot(t,x1)
xlabel('time(sec)')
ylabel('amplitude')
title('input signal of sinosoidal of 10Hz')
subplot(2,1,2)
plot(t,y1)
xlabel('time(sec)')
title('output signal filted with butterworth low pass at 25Hz')
ylabel('amplitude')

%y1=filtfilt(num,den,x1);

figure
plot(t,x1,'r')
hold on
plot(t,y1,'g')
xlabel('time(sec)')
ylabel('amplitude')
legend('input signal','output signal')
title('filtfilt function with no tim shift')


nfft = 2^10;
wndo = nfft;
ovlp = nfft/2;
u=x1;
y=y1;
[Suu,fr] = cpsd(u,u,wndo,ovlp,nfft,fs);
%[Snn,fr] = cpsd(n,n,wndo,ovlp,nfft,fs);
[Syy,fr] = cpsd(y,y,wndo,ovlp,nfft,fs);
%[Sun,fr] = cpsd(u,n,wndo,ovlp,nfft,fs);
```

```
[Syu,fr] = cpsd(y,u,wndo,ovlp,nfft,fs);
[Suy,fr] = cpsd(u,y,wndo,ovlp,nfft,fs);
%[Syn,fr] = cpsd(y,n,wndo,ovlp,nfft,fs);
H1 = Syu ./ Suu;
H2 = Syy ./ Suy;
H = squeeze(freqresp(plant,2*pi*fr));
gamma1 = (Syu .* Suy) ./ (Suu .* Syy);
gamma2 = mscohere(u,y,wndo,ovlp,nfft,fs);

figure
semilogx(fr,gamma1,'b');
grid on
xlabel('frequency(Hz)')
ylabel('coherence')
title('coherence of output filted by 25Hz')


%1G test and chapter 4

N=40000;
Gtest00=data01(5000:N,1:3);
Gtest01=data01(5000:N,7:9);
N=40000;
fs=200;
ts=1/fs;
t=[5000:N]*ts;
figure
plot(t,Gtest00(:,1),'r')
hold on
plot(t,Gtest00(:,2),'b')
hold on
plot(t,Gtest00(:,3),'y')
title('raw data of acc 00')

figure
plot(t,Gtest01(:,1),'r')
hold on
plot(t,Gtest01(:,2),'b')
hold on
plot(t,Gtest01(:,3),'y')
title('raw data of acc 01')


% low pass filter without  mean zero
[num,den]=butter(6,0.1); %fc=10
for i=1:3
    Gtest00(:,i)=filtfilt(num,den,Gtest00(:,i));
    Gtest01(:,i)=filtfilt(num,den,Gtest01(:,i));
end
figure
plot(t,Gtest00(:,1),'r')
hold on
plot(t,Gtest00(:,2),'b')
hold on
plot(t,Gtest00(:,3),'y')
```

```
title('6th order filter 10Hz=fc for acc 00')

figure
plot(t,Gtest01(:,1),'r')
hold on
plot(t,Gtest01(:,2),'b')
hold on
plot(t,Gtest01(:,3),'y')
title('6th order filter 10Hz=fc for acc 01')

%% just tried to see the result of the gravity
G=zeros(N,1);
for i=1:N
    G(i)=Gtest00(i,1)^2+Gtest00(i,2)^2+Gtest00(i,3)^2;
    G(i)=sqrt(G(i));
end
figure
plot(t,G) %% plot the square result of the data

%% STFT of each 1,2,3 graph
nfft=1000;
wndo=nfft;
ovlp=wndo/2;
fr=fs/nfft;
[S001,F,T] = spectrogram(Gtest00(:,1),wndo,ovlp,nfft,fs);
[S002,F,T] = spectrogram(Gtest00(:,2),wndo,ovlp,nfft,fs);
[S003,F,T] = spectrogram(Gtest00(:,3),wndo,ovlp,nfft,fs);

figure
h=surf(T,F(1:25),abs(S001(1:25,:)),'EdgeColor','none')
title('acc00 x axis')
xlabel('time')
ylabel('frequency(Hz)')
figure
surf(T,F(1:25),abs(S002(1:25,:)),'EdgeColor','none')
title('acc00 y axis')
xlabel('time')
ylabel('frequency(Hz)')
figure
surf(T,F(1:25),abs(S003(1:25,:)),'EdgeColor','none')
title('acc00 z axis')
xlabel('time')
ylabel('frequency(Hz)')
%% STFT of each 7,8,9 graph
    nfft=1000;
wndo=nfft;
ovlp=wndo/2;
fr=fs/nfft;
f=fr*[1:N-1];
[S011,F,T] = spectrogram(Gtest01(:,1),wndo,ovlp,nfft,fs);
[S012,F,T] = spectrogram(Gtest01(:,2),wndo,ovlp,nfft,fs);
[S013,F,T] = spectrogram(Gtest01(:,3),wndo,ovlp,nfft,fs);

figure
h=surf(T,F(1:25),abs(S011(1:25,:)),'EdgeColor','none')
title('acc00 x axis')
```

```
xlabel('time')
ylabel('frequency(Hz)')
figure
surf(T,F(1:25),abs(S012(1:25,:)),'EdgeColor','none')
title('acc00 y axis')
xlabel('time')
ylabel('frequency(Hz)')
figure
surf(T,F(1:25),abs(S013(1:25,:)),'EdgeColor','none')
title('acc00 z axis')
xlabel('time')
ylabel('frequency(Hz)')
%%mscohere of these 9 combination

[Cxx,F] = mscohere(Gtest00(:,1),Gtest01(:,1),wndo,ovlp,nfft,fs,'onesided');
[Cxy,F] = mscohere(Gtest00(:,1),Gtest01(:,2),wndo,ovlp,nfft,fs,'onesided');
[Cxz,F] = mscohere(Gtest00(:,1),Gtest01(:,3),wndo,ovlp,nfft,fs,'onesided');
figure
plot(F,Cxx)
figure
plot(F,Cxy)
figure
plot(F,Cxz)

%time frequency method
nfft=1000;
wndo=rectwin(1000);
ovlp=900;
Block size B=10,000
increment 100 rectangular window with weighted average
l=1;
figure
for j=1:3
    for k=1:3

        Gamma=zeros(251,nfft/2+1);
        gamma=zeros(90,nfft/2+1); %will store the time-frequency coherence
        strt=1;
        ed=10000;

        for i=1:251

            strtW=strt;
            edW=strtW+1000;

            Gxy=zeros(90,nfft/2+1);
            Gyx=zeros(90,nfft/2+1);
            Gxx=zeros(90,nfft/2+1);
            Gyy=zeros(90,nfft/2+1);
            window size 1000, incremenet 100(overlapping 90%) and total size
of the block = 10,000
            for o=1:90

                X=fft(Gtest00(strtW:edW,j));
                Y=fft(Gtest01(strtW:edW,k));
```

```
                X=X(1:nfft/2+1);
                Y=Y(1:nfft/2+1);
                X(2:nfft/2)=2*X(2:nfft/2);
                Y(2:nfft/2)=2*Y(2:nfft/2);

                Gxy(o,:)=X.*conj(Y);
                Gyx(o,:)=Y.*conj(X);
                Gxx(o,:)=X.*conj(X);
                Gyy(o,:)=Y.*conj(Y);

                strtW=strtW+100;
                edW=edW+100;
            end

            weightV=[[1:45] [45:-1:1]];
            AvGxy=sum(weightV*Gxy,1)/sum(weightV);
            AvGyx=sum(weightV*Gyx,1)/sum(weightV);
            AvGxx=sum(weightV*Gxx,1)/sum(weightV);
            AvGyy=sum(weightV*Gyy,1)/sum(weightV);

            gamma=(AvGyx .* AvGxy) ./ (AvGxx .* AvGyy);
            Gamma(i,:)=gamma;
            strt=strt+100;
            ed=ed+100;


        end

        ti=sprintf('coherence between acc0 %d and acc1 %d',j,k);
        Tu=[1:251];     %time index doesnot mean the time
        subtightplot(3,3,l,[0.1,0.05,0.1])
        l=l+1;
        Fu=[1:501]*100/500;
        surf(Tu,Fu,Gamma','EdgeColor','none')
        axis([1 251 1 15 0 1])
        xlabel('time index')
        ylabel('frequency')
        zlabel('coherence')
        title(ti)
                colorbar

    end
end



figure
A=mscohere(Gtest00(1:10000,1),Gtest01(1:10000,1),wndo,ovlp,nfft,fs,'twosided'
);

l=1;
for j=1:3
    for k=1:3
        Mxx=zeros(251,nfft/2+1);
```

```
        %gamma1=zeros(251,nfft/2+1);
        strt=1;
        ed=10000;
        for i=1:251
            [Mxx(i,:),F] =
mscohere(Gtest00(strt:ed,j),Gtest01(strt:ed,k),wndo,ovlp,nfft,fs,'onesided');
%
%             Pxx=pwelch(Gtest00(strt:ed,j),wndo,ovlp,nfft,fs,'onesided') ;
%             Pyy=pwelch(Gtest01(strt:ed,k),wndo,ovlp,nfft,fs,'onesided');
%
Pxy=cpsd(Gtest00(strt:ed,j),Gtest01(strt:ed,k),wndo,ovlp,nfft,fs,'onesided');
%
Pyx=cpsd(Gtest01(strt:ed,k),Gtest00(strt:ed,j),wndo,ovlp,nfft,fs,'onesided');
%             gamma1(i,:) = (Pyx .* Pxy) ./ (Pxx .* Pyy);
            strt=strt+100;
            ed=ed+100;
        end


        ti=sprintf('coherence between acc0 %d and acc1 %d',j,k);
        Tu=[1:251];
%         figure
%         %surf(t,F(5:501),Mxx(:,5:501)','EdgeColor','none')
%         surf(Tu,F(5:75),Mxx(:,5:75)','EdgeColor','none')
%         title(ti)
%
        subtightplot(3,3,l,[0.1,0.05,0.1])
        l=l+1;
        Fu=[1:501]*100/500;
        surf(Tu,Fu,Mxx','EdgeColor','none')
        axis([1 251 1 15 0 1])
        xlabel('time index')
        ylabel('frequency')
        zlabel('coherence')
        title(ti)
        %         colorbar

    end
end

{
Pxx=fft(Gtest00(:,1));
Pyy=fft(Gtest01(:,2));
Pxy=Pxx.*Pyy;
Pyx=Pyy.*Pxx;
Pxx=Pxx.*Pxx;
Pyy=Pyy.*Pyy;
gamma1 = (Pyx .* Pyx) ./ (Pyy .* Pxx);
figure
plot(fr,gamma1)
}
```